Pulsar Wind Nebulae

Niccolo' Bucciantini

INAF - Osservatorio di Arcetri

INFN - Sezione di Firenze

Outline

PWNe & SNRs introduction

PSR wind and injection

One-zone model and SED fitting

MHD models and X-ray maps

News in MHD modelling

Evolution of PWNe and BSPWNe

Supernova Remnants

SNRs are originated from the death of a star in a Supernova Explosion

Plerions
center filled morphology

Shell

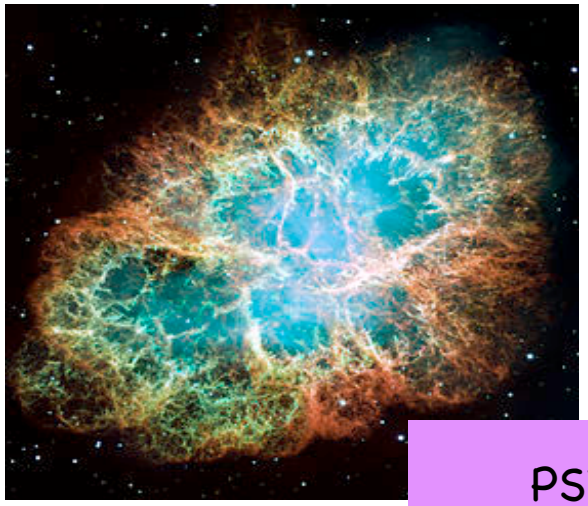

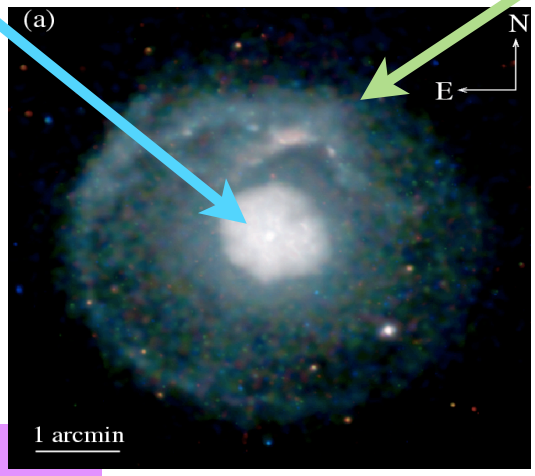

PSR

Pulsar Wind Nebulae

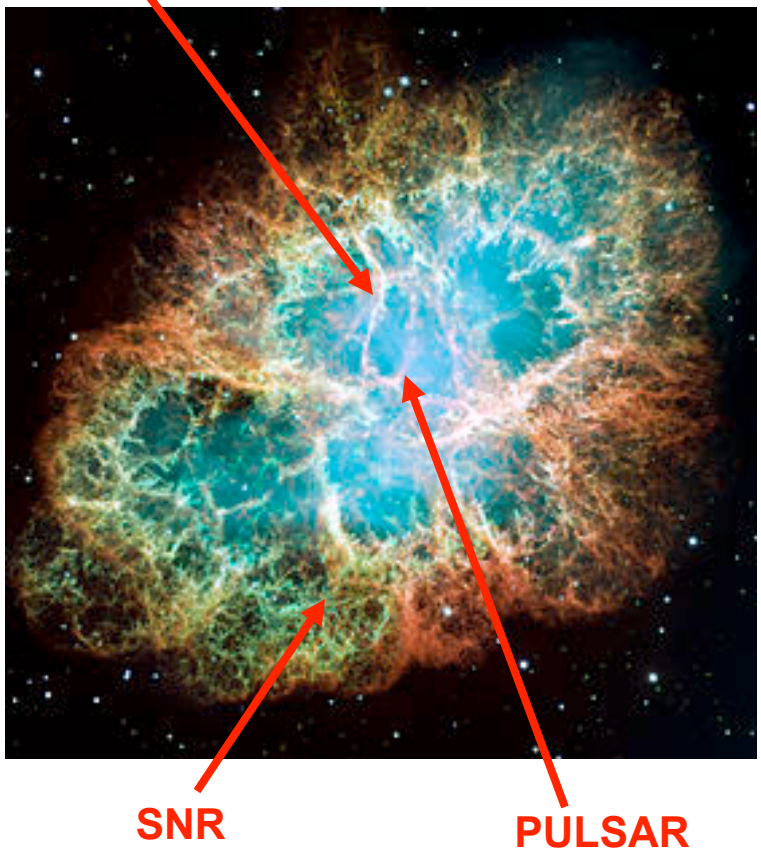

- **PWNe are hot bubbles of relativistic particles and magnetic field emitting non-thermal radiation.**
- **Originated by the interaction of the ultra-relativistic magnetized pulsar wind with the expanding SNR (or with the ISM)**
- **Galactic accelerators. The only place where we can study the properties of relativistic shocks (as in GRBs and AGNs**
- **Allow us to investigate the dynamics of relativistic outflows**

PWNe Spectrum

Low energy break

High energy break

MeV cutoff

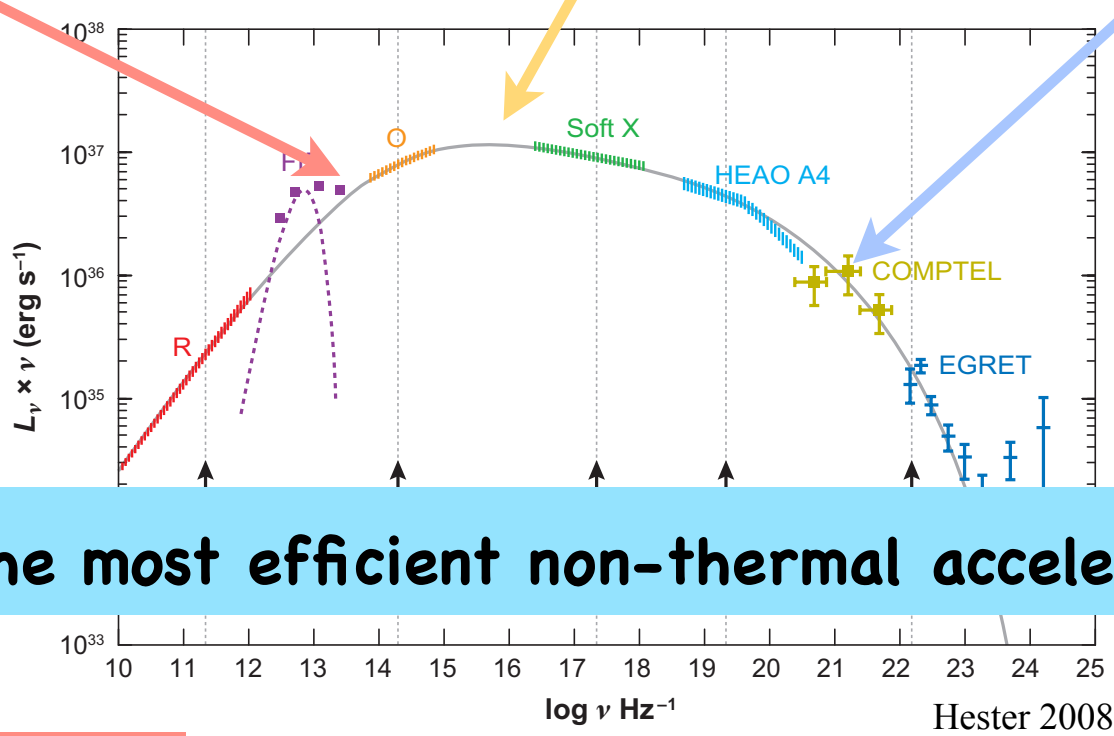

Hester 2008

The most efficient non-thermal accelerator.

Injection break

Synchr. cooling

Acceler. cutoff

PWNe & Synchrotron

Synchrotron was recognized for the first time in astrophysics by

Woltjer in 1958 from the high optical polarization measured by Oort in the Crab nebula

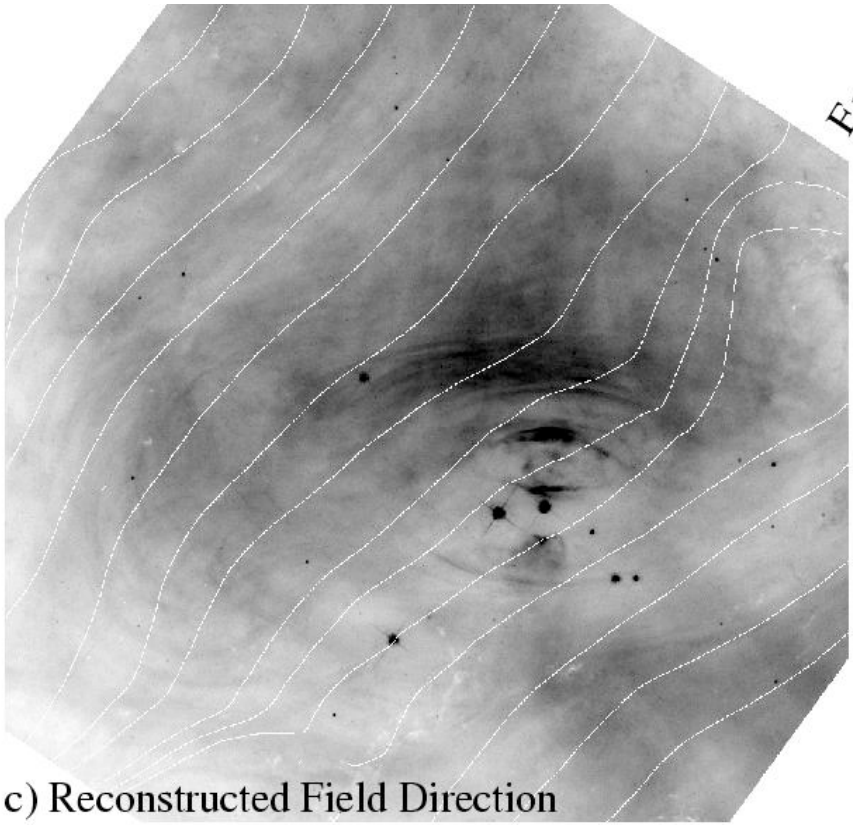

Optical however suffers from large foreground effects from dust (in induces also circular polarization)

Injection

Crab Nebula: Remnant of an Exploded Star (Supernova)

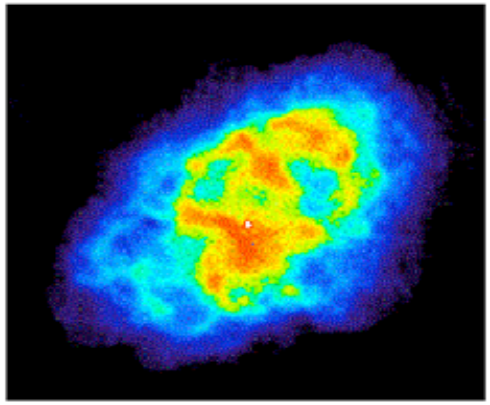

Radio wave (VLA)

Infrared radiation (Spitzer)

Visible light (Hubble)

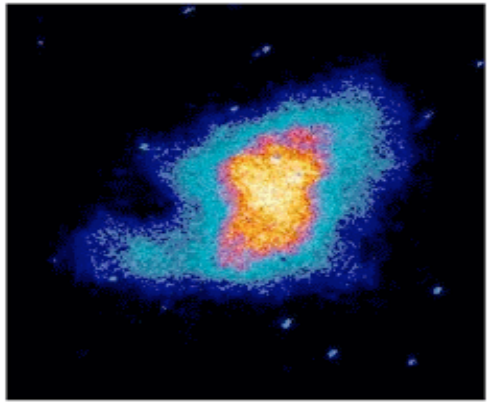

Ultraviolet radiation (Astro–1)

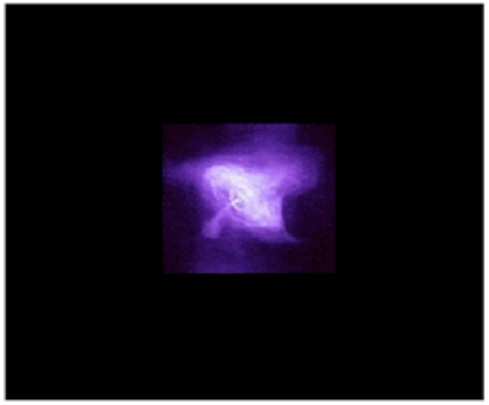

Low–energy X–ray (Chandra)

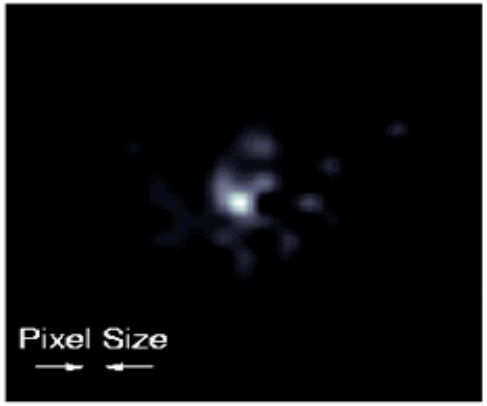

High–energy X–ray (HEFT)
***** 15 min exposure *****

The pulsar magnetosphere

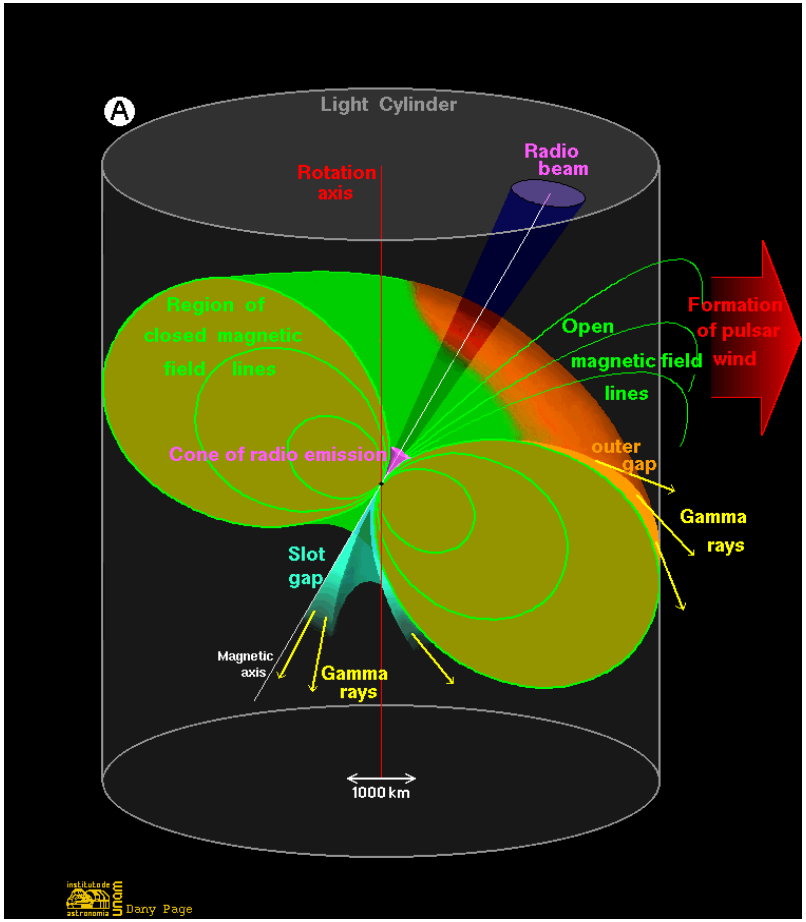

R ~ 10 km
P ~ 0.001–1 sec
B ~ 10^{8-12} G

Strong unscreened electric field
Pair cascade

Acceleration of particle pair plasma-ions from the surface:
Initial Lorentz factor ~ 100
Cold wind (Sync. losses)

The PSR wind

Force-free (Contopulos et al 1999, Gruzinov 2005, Spitkovsky 2006, Timokhin 2006, ...)
RMHD (Bogovalov 2001, Komissarov 2006, Bucciantini et al. 2006)

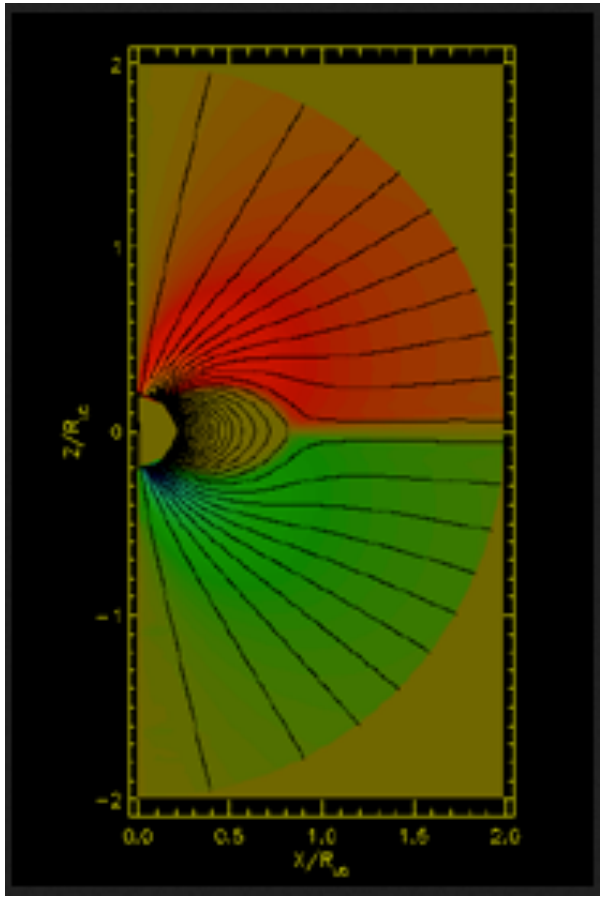

Outside the Light Cylinder the field become progressively more toroidal

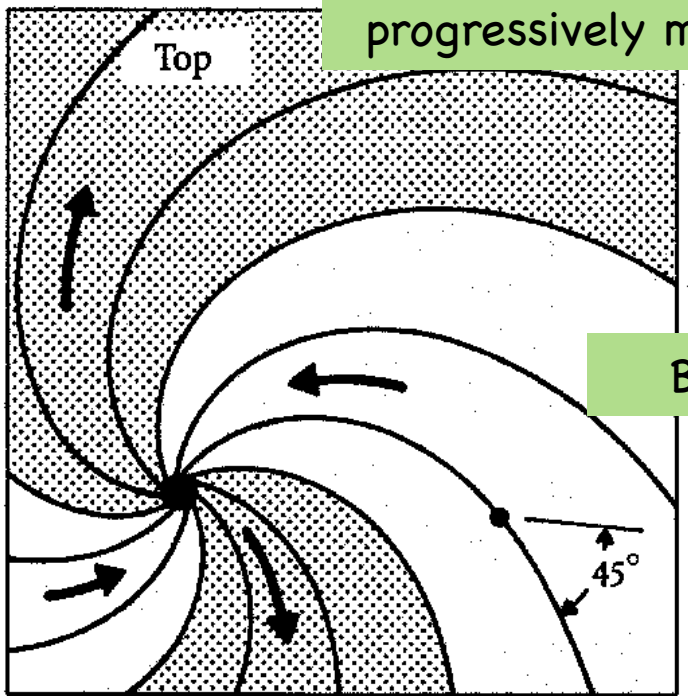

$B_t/B_r = R/R_{LC}$

The striped wind

Magnetic inclination give rise to a striped wind

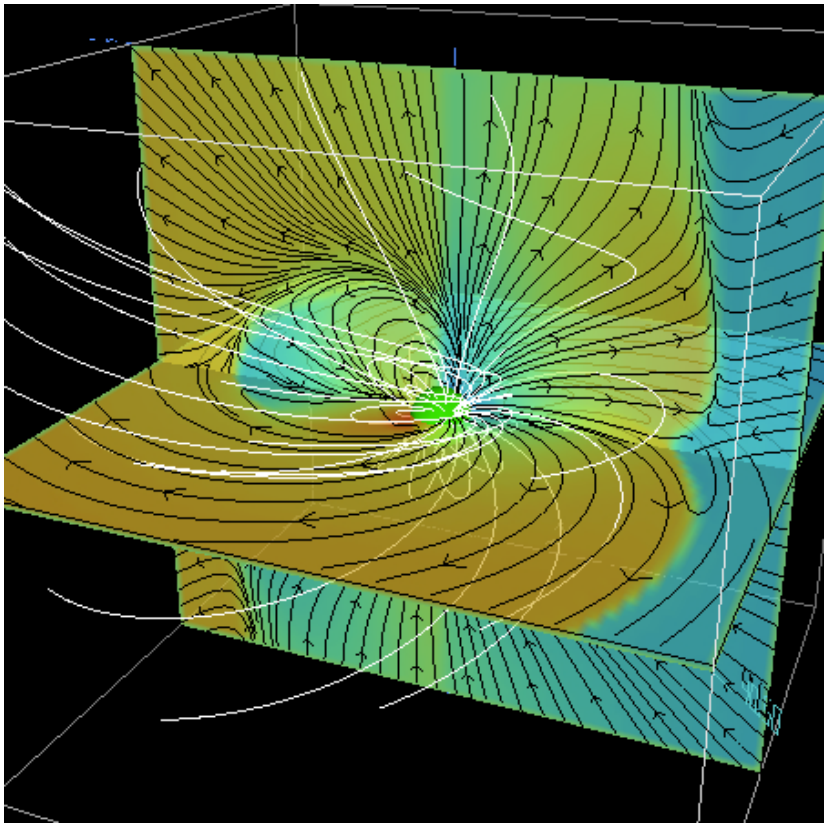

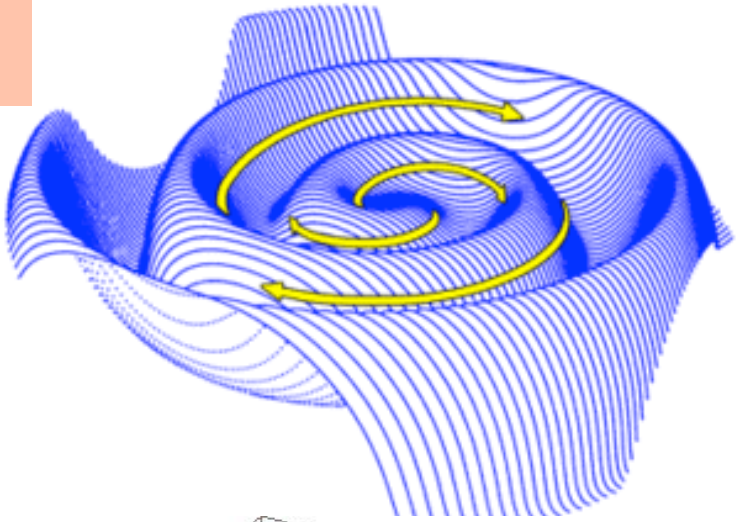

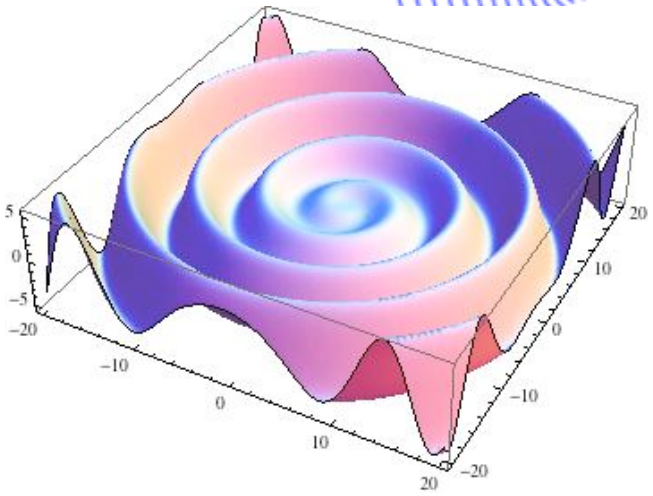

Energetics - Termination Shock

Energetics

$$M_{\rm ej} V_{\rm pwn}^2 \simeq E_{\rm rot} = \frac{I_{\rm NS}}{2}\Omega_o^2$$

$$V_{\rm pwn} \simeq 10^8 \left(\frac{10 M_\odot}{M_{\rm ej}}\right)^{1/2} \left(\frac{\Omega_o}{600}\right)$$

A shock must form

Pressure equilibrium

$$\frac{\dot{E}}{4\pi c R_{\rm TS}^2} \approx P_{\rm pwn} \approx \frac{E_{\rm pwn}}{R_{\rm pwn}^3} \approx \frac{\dot{E} t_{\rm pwn}}{R_{\rm pwn}^3} \quad \Rightarrow \quad R_{\rm TS} \approx R_{\rm pwn}\sqrt{\frac{V_{\rm pwn}}{c}}$$

Shock Jump Conditions

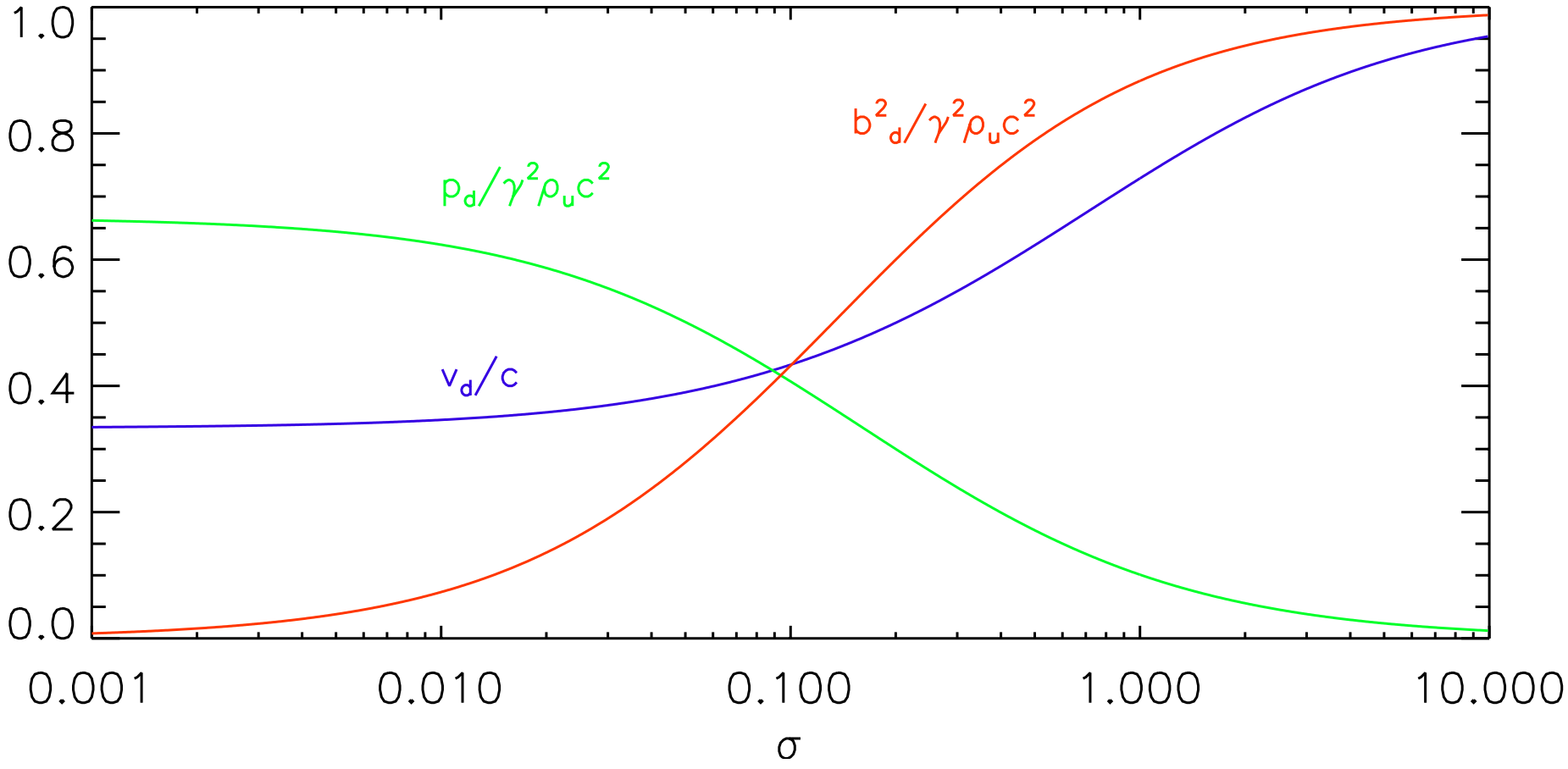

Pair Plasma

Perpendicular relativistic shock - Superluminal

Maxwellian at low energies

Evidence for non-thermal tail only for subluminal shock

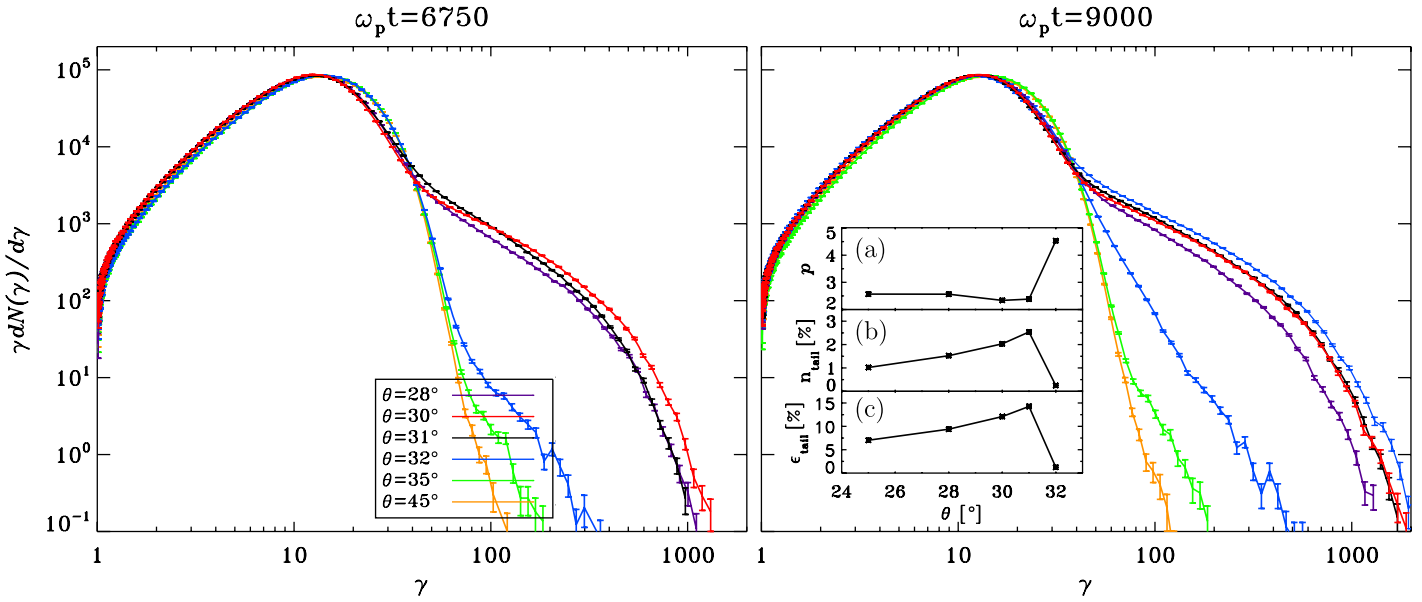

Spitkovsky 2006

Striped -Wind

In a striped wind reconnection of alternating fields can accelerate particles

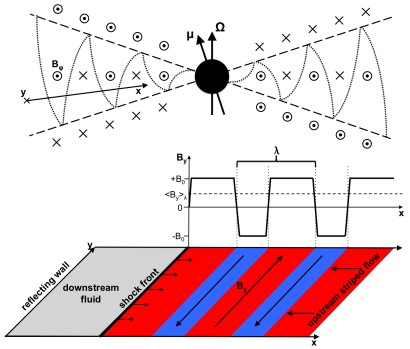

Sironi & Spitkovsky 2007

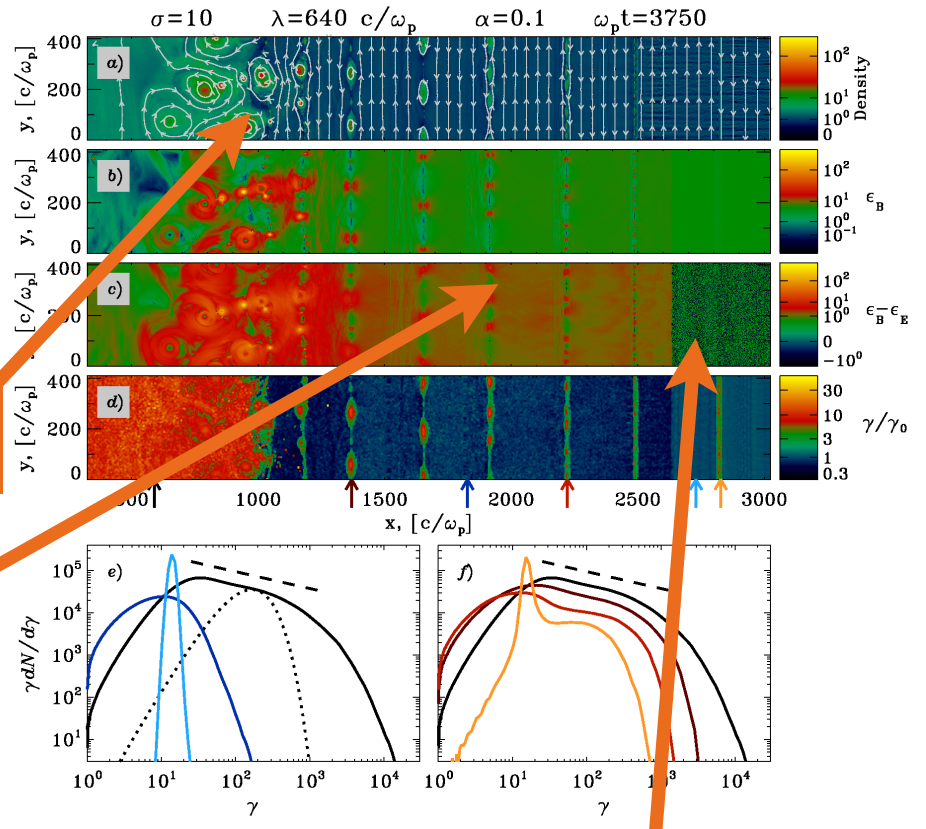

HD shock

Tearing modes reconnection

Hard spectrum

Fast-magnetosonic precursor

Striped -Wind

Reconnection in a striped wind produces hard spectra - N(E)~E^{-1}

The hard spectrum extends for an energy range from γmin ≃ γ$_0$ to γmax ≃ γ$_0$ σ$^{1/(2-p)}$

High magnetization σ >= 30 and multiplicity >= 10^8

Low γ$_0$ ~ 10

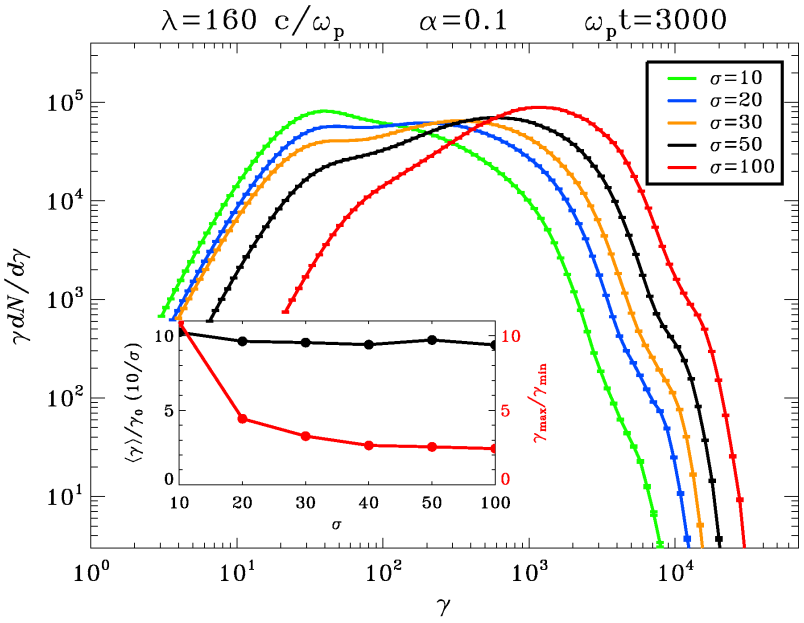

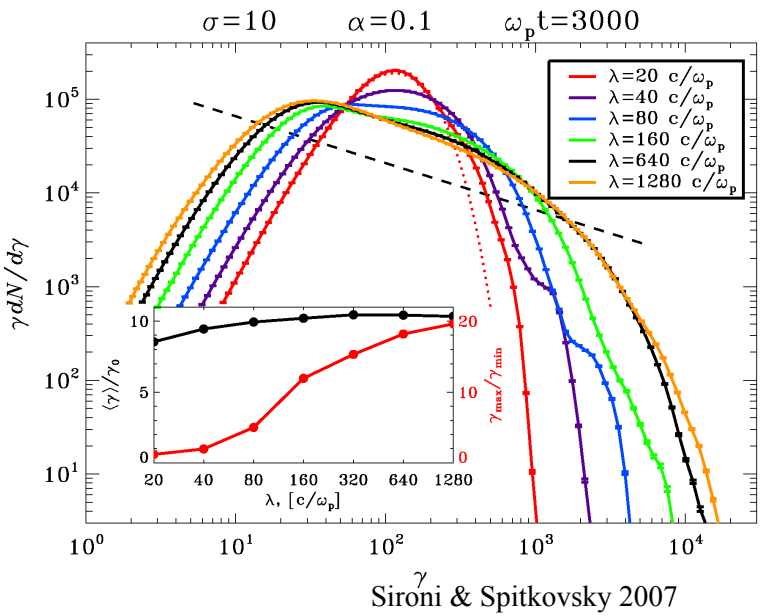

Sironi & Spitkovsky 2007

Which Acceleration?

FERMI MECHANISM

(Spitkovsky09) **MAGNETIZATION (σ<0.001)**

DRIVEN MAGNETIC RECONNECTION

(Sironi&Spitkovsky11) **PULSAR MULTIPLICITY (k>10^8)**

RESONANT CYCLOTRON ABSORPTION

(Amato&Arons06)

PRESENCE OF IONS AND MULTIPLICITY (K<10^4)

MAGNETIZATION

$$\dot{E}_R = \kappa\ \dot{N}_{GJ}\ m_\pm\ c^2\ \Gamma_{wind} \left(1 + \frac{\xi m_i}{\kappa m_\pm}\right)(1+\sigma)$$

PAIRS **IONS**

$$\sigma = \frac{B^2}{4\pi\, m_{eff}\, n_{eff}\, c^2\, \Gamma_{wind}^2}$$

Cartoon

Outgoing Shell
V_{sn} ~ 0.003-0.01c
SNR Shell

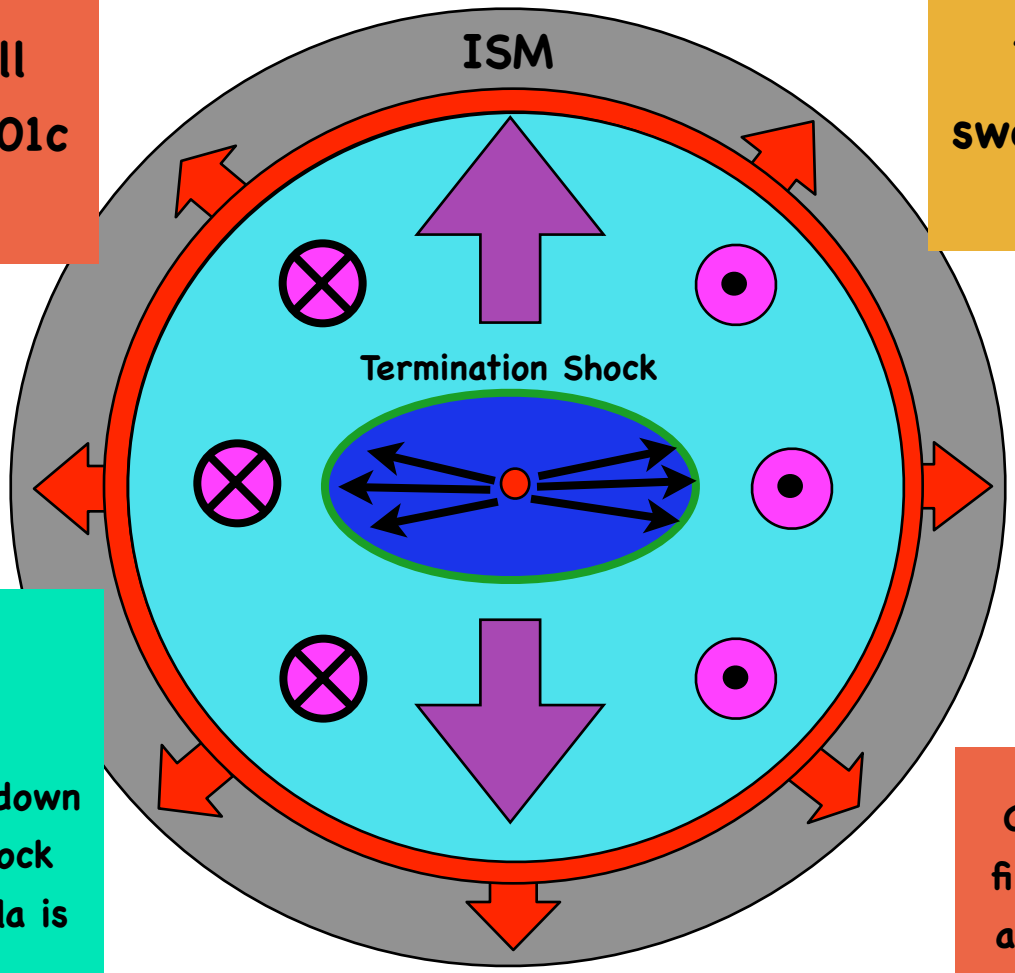

The cavity is swept by the PRS wind

$V_{sn} << V_{wind}$

The wind is slowed down in a termination shock
A pulsar wind nebula is formed

Compressed magnetic field is mostly toroidal and presses along the axis

Radio Polarization of PWNe

High Polarization 30-40%=> Synchrotron

Toroidal Magnetic Field

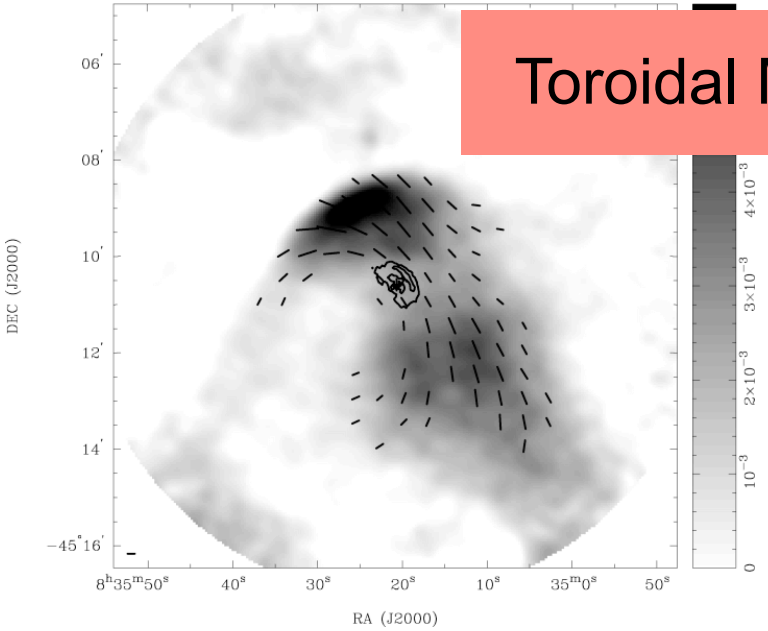

Vela, Dodson et al 03

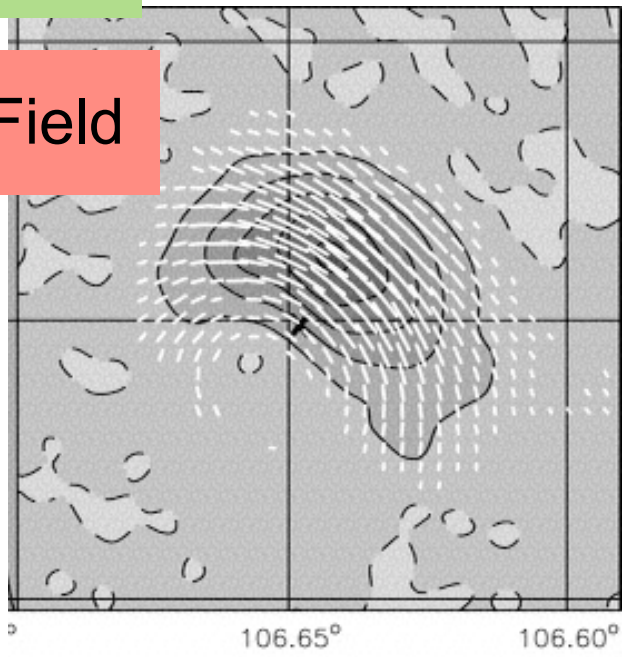

G106.6+29, Kothes et al 06

Not all PWNe have clearly defined polarization geometry

One-Zone model

The PWN is treated as a uniform expanding bubble, with no internal gradients

At each time one define various quant
The nebular radius-size
The nebular magnetic field

One can then follow the evolution
emitting particles injected inside the r
and subject to losses, and compu
emission

$$\frac{\mathrm{d}E(t)}{\mathrm{d}t} = -\frac{\dot{R}(t)}{R(t)}E(t) - \frac{4\sigma_{\mathrm{t}}}{3m^2c^3}E^2(t)\left(\frac{B(t)^2}{8\pi}\right.$$

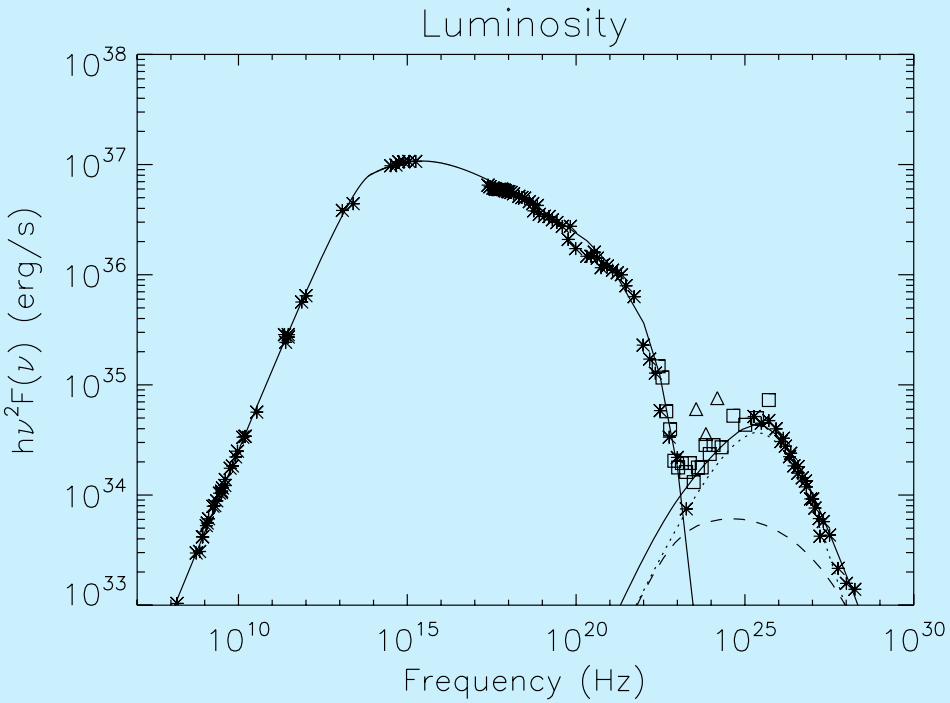

Radio VS Optical VS X-ray

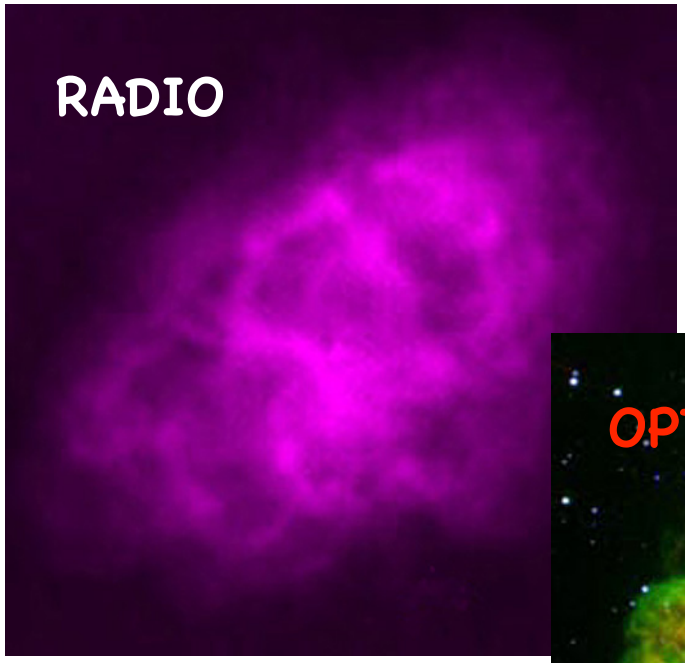

Non-thermal

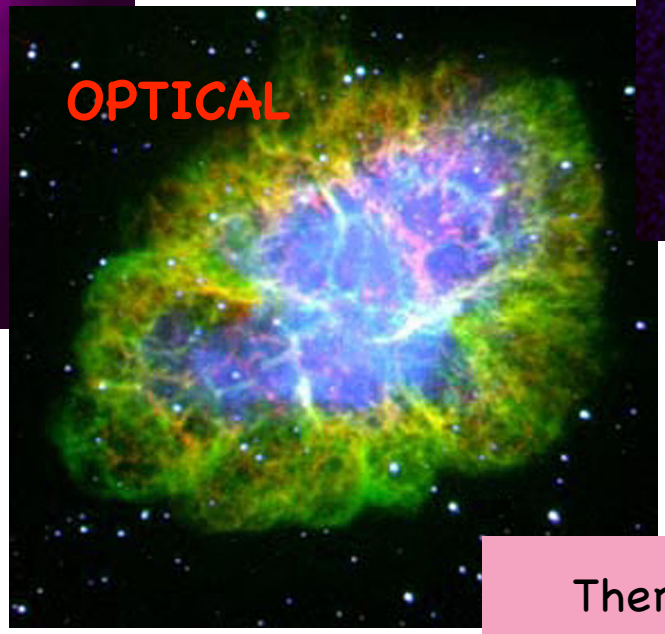

Thermal line emission

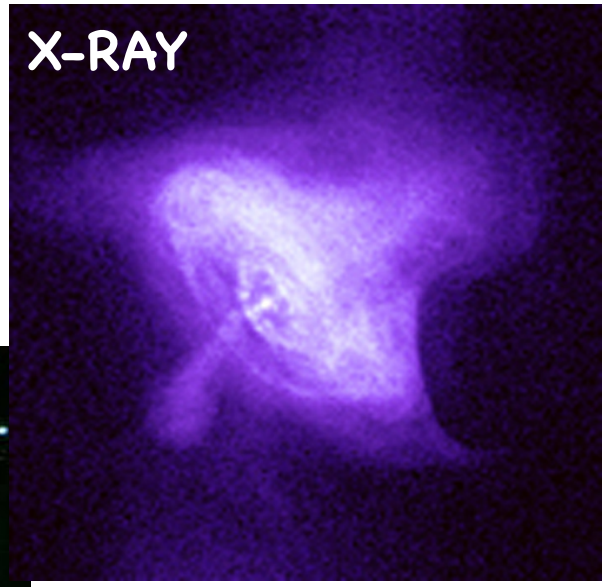

Non-thermal

Jet-torus structure: Chandra X-ray

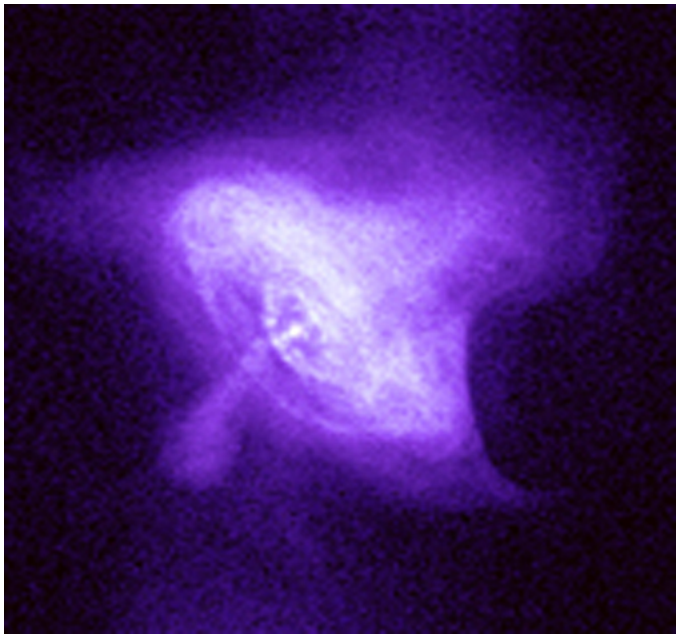

Crab

Vela

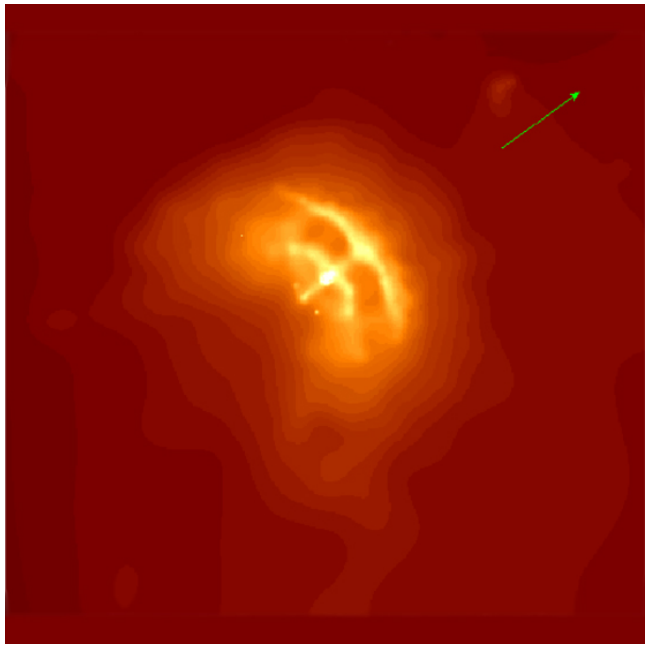

- Crab Nebula (*Weisskopf et al., 2000; Hester et al., 2002*)
- Vela pulsar (*Helfand et al., 2001; Pavlov et al., 2003*)

How common is the jet-torus

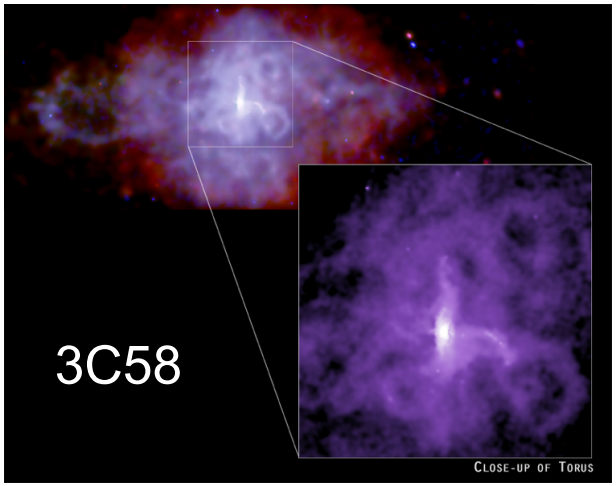

Jet perpendicular to the torus
Jet variability

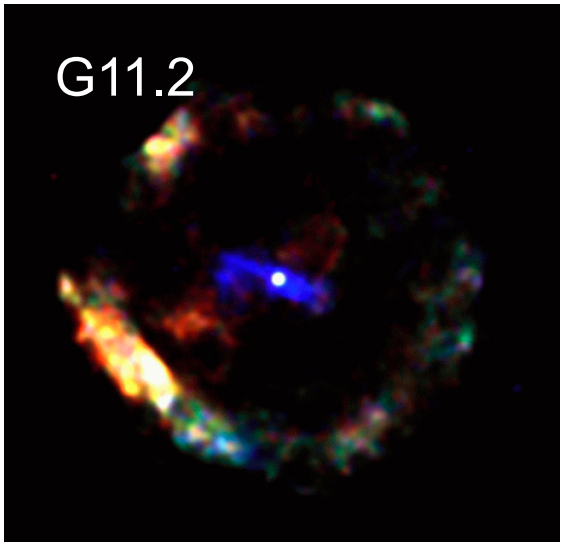

Inner ring

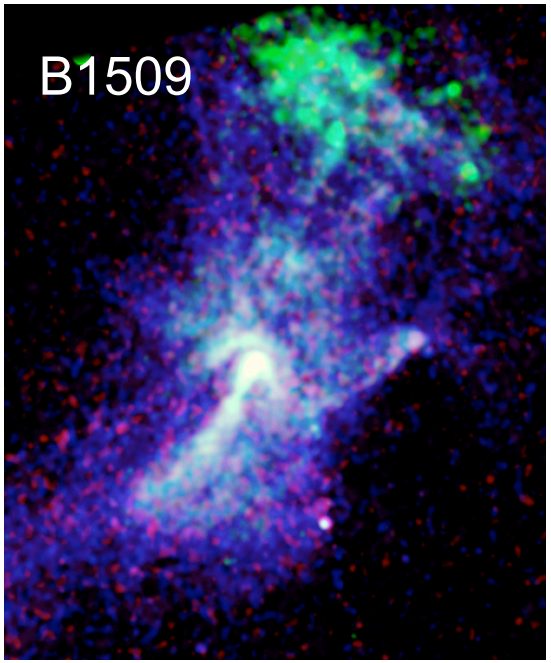

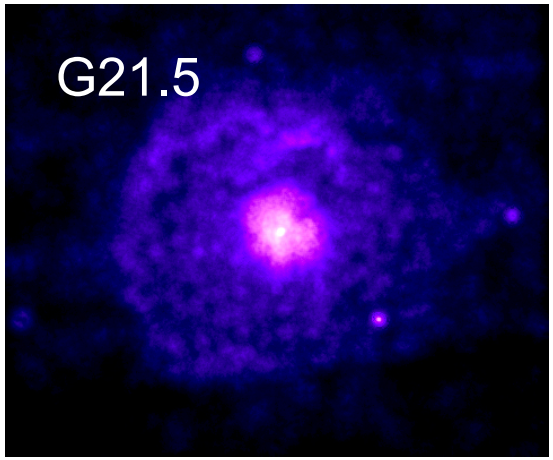

A case for MHD

Why an MHD description?

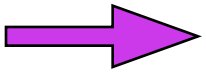

MHD is "simple"

Larmor radii << nebular radius (advective regime)
Energy losses are negligible (radio particles dominate)
Almost pure pair plasma (no dispersive-plasma effects)
Interested in long evolutionary timescales

Particles are accelerated with high efficiency
Short time-scale variation at very high energies

PWNe MHD theory

Theoretical model for PWNe - quasi steady-state

Expansion speed << sound speed

The wind terminates with a strong MHD shock

- Particles are accelerated at TS
- Relativistic MHD flow in the PWN region
- Synchrotron losses inside the nebula
- Wind parameters derived by comparison with observations:

$$R_{TS} = 3\times10^{17}\,cm, \quad L = 5\times10^{38}\,erg/s, \quad \gamma = 3\times10^{6}, \quad \sigma = 3\times10^{-3}$$

Jet-torus structure: theory

The torus could be explained with a higher equatorial energy flux as expected by the PSR wind models

The torus is much brighter on the front side - strong doppler boosting v~ 0.5c

There is not collimated outflows in the PSR wind to make the jet

$$\gamma >> 1 \Rightarrow \rho_q \bar{E} + \vec{j} \times \bar{B} \approx 0$$

The jet is due to post-shock collimation

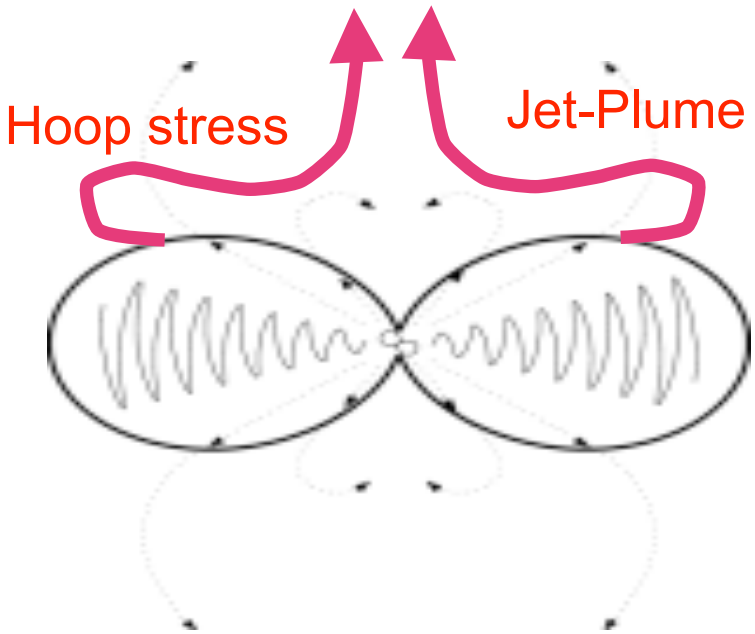

TS structure and flow pattern

The wind anisotropy shapes the TS structure. Downstream flow - equatorial collimation due to the TS shape:

A: ultrarelativistic pulsar wind

B: subsonic equatorial outflow

C: supersonic equatorial funnel

D: super-fastmagnetosonic flow

a: termination shock front

b: rim shock

c: fastmagnetosonic surface

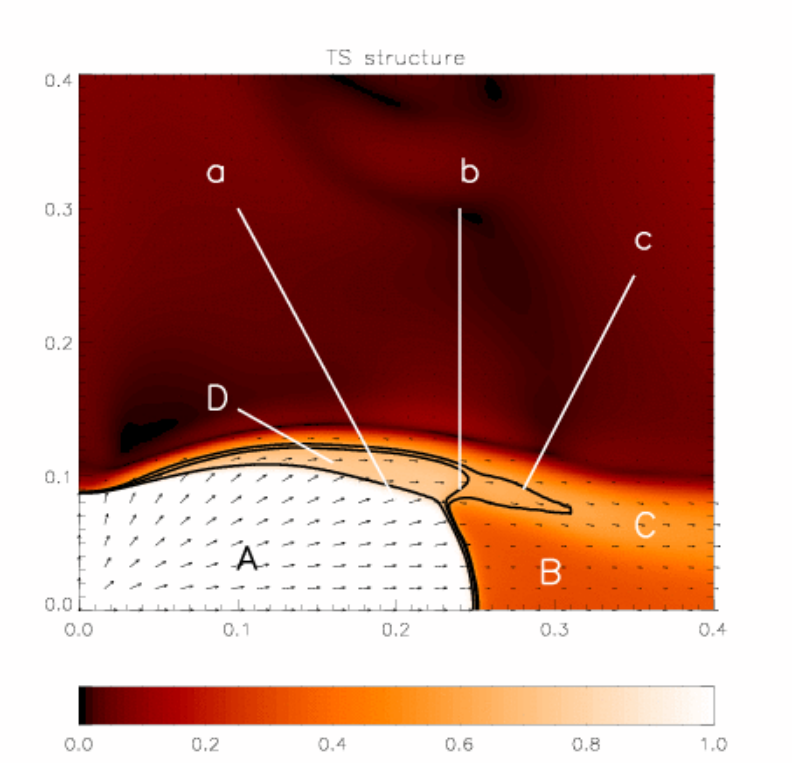

Dynamics is 2D

- **Initial magnetic field with a narrow equatorial neutral sheet**
- **Dissipation in a striped wind**

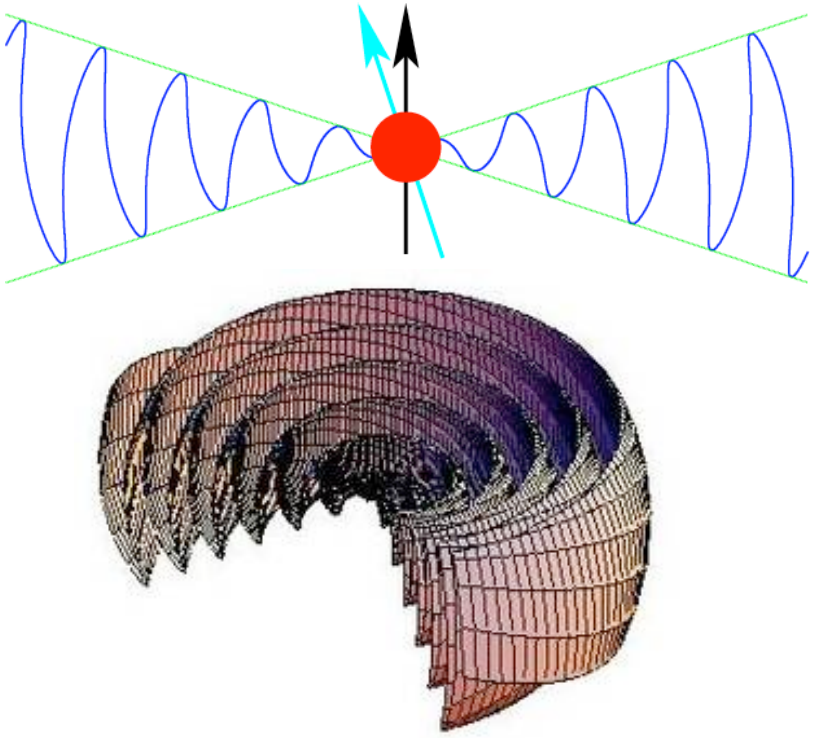

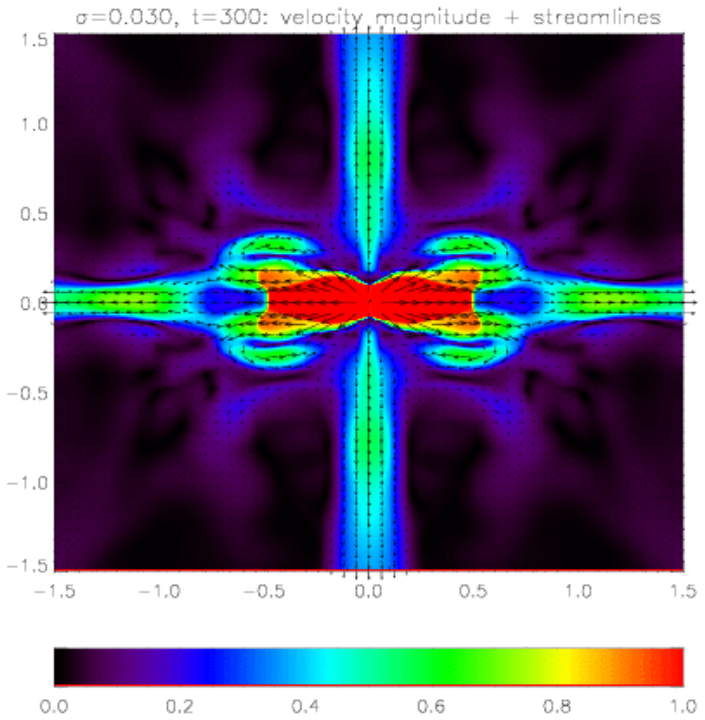

Synchrotron Dopple Boosting

Truncated power-law distribution

$$f(\epsilon) = \frac{K_p}{4\pi}\frac{p}{mc^2}\epsilon^{-(2\alpha+1)}, \quad \epsilon < \epsilon_\infty,$$

Comoving emissivity

$$j'_\nu(\nu', \boldsymbol{n}') = Cp|\boldsymbol{B}' \times \boldsymbol{n}'|^{\alpha+1}\nu'^{-\alpha}$$

Lab emissivity

$$j_\nu(\nu, \boldsymbol{n}) = \begin{cases} Cp\,|\boldsymbol{B}' \times \boldsymbol{n}'|^{\alpha+1} D^{\alpha+2}\nu^{-\alpha}, & \nu_\infty \geq \nu \\ 0, & \nu_\infty < \nu. \end{cases}$$

$$D = \frac{1}{\gamma(1 - \boldsymbol{\beta}\cdot\boldsymbol{n})}$$

$$\nu_\infty \equiv D\nu'_c(\epsilon_\infty) = D\frac{3e}{4\pi mc}|\boldsymbol{B}' \times \boldsymbol{n}'|\epsilon_\infty^2,$$

$$\boldsymbol{n}' = D\left[\boldsymbol{n} + \left(\frac{\gamma^2}{\gamma+1}\boldsymbol{\beta}\cdot\boldsymbol{n} - \gamma\right)\boldsymbol{\beta}\right]$$

$$\boldsymbol{B}' = \frac{1}{\gamma}\left[\boldsymbol{B} + \frac{\gamma^2}{\gamma+1}(\boldsymbol{\beta}\cdot\boldsymbol{B})\boldsymbol{\beta}\right]$$

MHD

Synchrotron Angle Swing

MHD

$$|\boldsymbol{B}' \times \boldsymbol{n}'| = \frac{1}{\gamma}\sqrt{B^2 - D^2(\boldsymbol{B}\cdot\boldsymbol{n})^2 + 2\gamma D(\boldsymbol{B}\cdot\boldsymbol{n})(\boldsymbol{\beta}\cdot\boldsymbol{B})},$$

Integration along the line of sight

$$I_\nu(\nu, Y, Z) = \int_{-\infty}^{\infty} j_\nu(\nu, X, Y, Z)\,\mathrm{d}X.$$

$$Q_\nu(\nu, Y, Z) = \frac{\alpha+1}{\alpha+5/3}\int_{-\infty}^{\infty} j_\nu(\nu, X, Y, Z)\cos 2\chi\,\mathrm{d}X,$$

$$U_\nu(\nu, Y, Z) = \frac{\alpha+1}{\alpha+5/3}\int_{-\infty}^{\infty} j_\nu(\nu, X, Y, Z)\sin 2\chi\,\mathrm{d}X,$$

Electric field

$$\boldsymbol{e} = \gamma\left[\boldsymbol{e}' - \frac{\gamma}{\gamma+1}(\boldsymbol{e}'\cdot\boldsymbol{\beta})\boldsymbol{\beta} - \boldsymbol{\beta}\times\boldsymbol{b}'\right]$$

$$\boldsymbol{e} \propto \boldsymbol{n}\times\boldsymbol{q}, \quad \boldsymbol{q} = \boldsymbol{B} + \boldsymbol{n}\times(\boldsymbol{\beta}\times\boldsymbol{B})$$

PA

$$\cos 2\chi = \frac{q_Y^2 - q_Z^2}{q_Y^2 + q_Z^2}, \quad \sin 2\chi = -\frac{2q_Y q_Z}{q_Y^2 + q_Z^2}.$$

Comparison with Observations

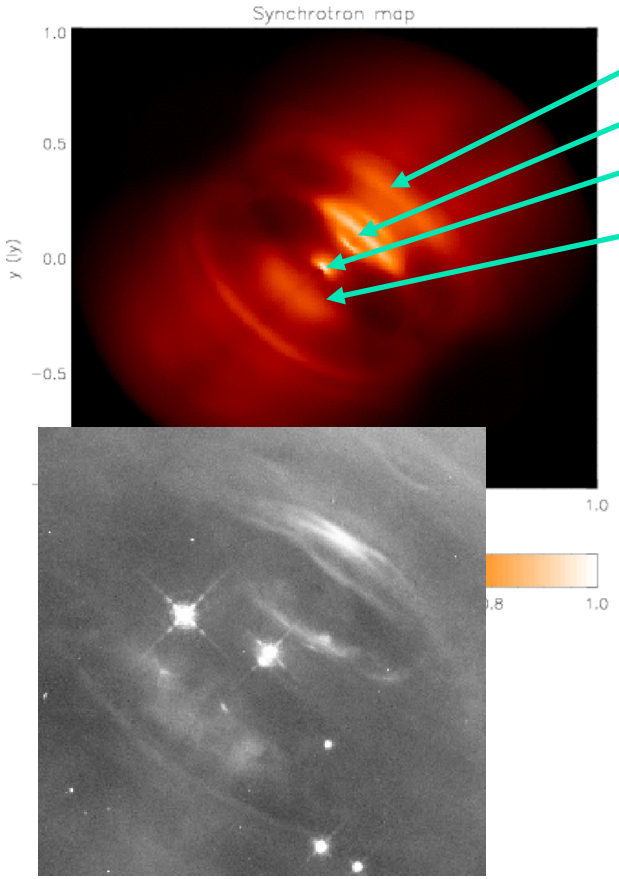

Hester et al. 1995

Main torus
Inner ring (wisps structure)
Knot
Back side of the inner ring

Each feature traces an emitting region

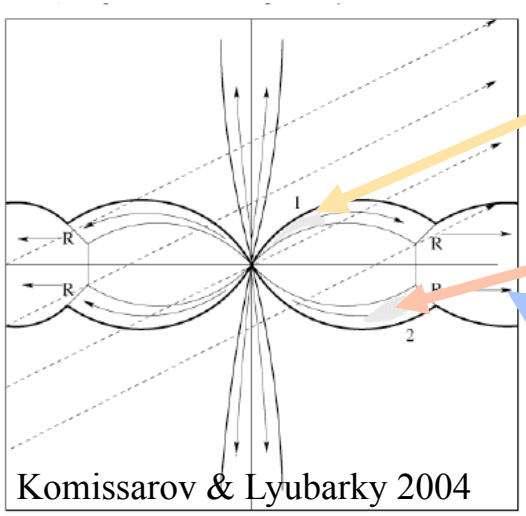

Komissarov & Lyubarky 2004

Knot

Ring

Torus

Comparison with Observations

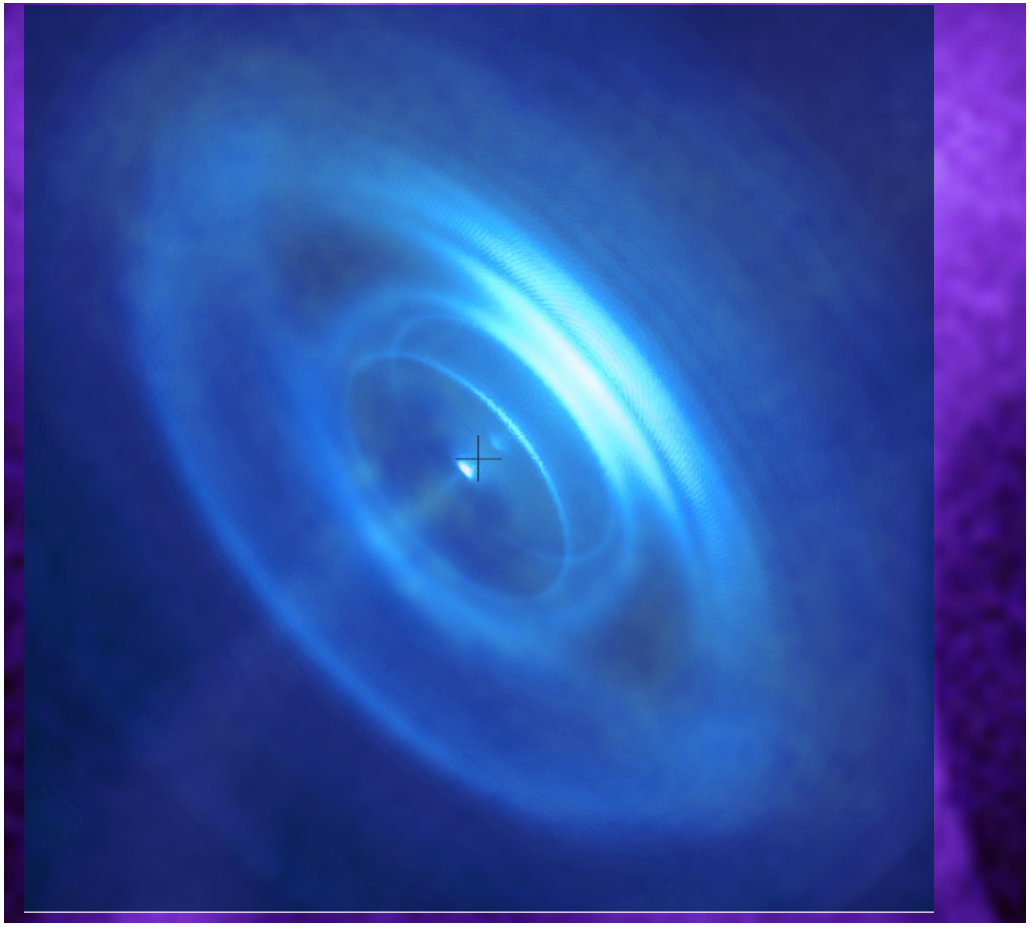

Time variability

Wisp moving outward
Year long limit cycle
Variability in the knot
Bubble in the jet v~ 0.6 c

Variability in the knot structure
Jet feature moving at 0.6 c

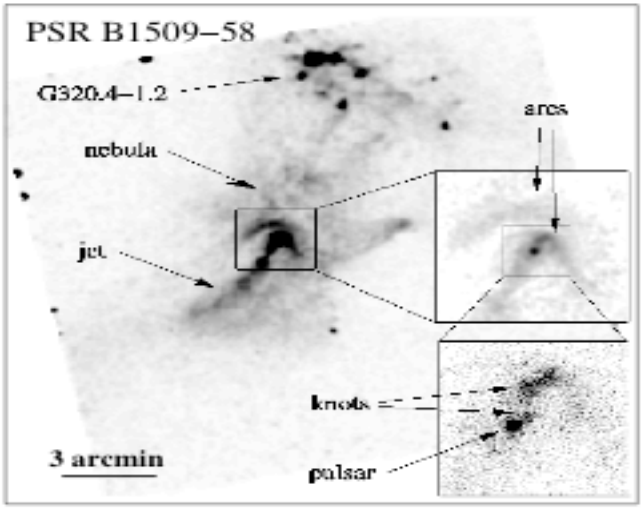

Slane 05, DeLaney 06

MHD variability - Flow

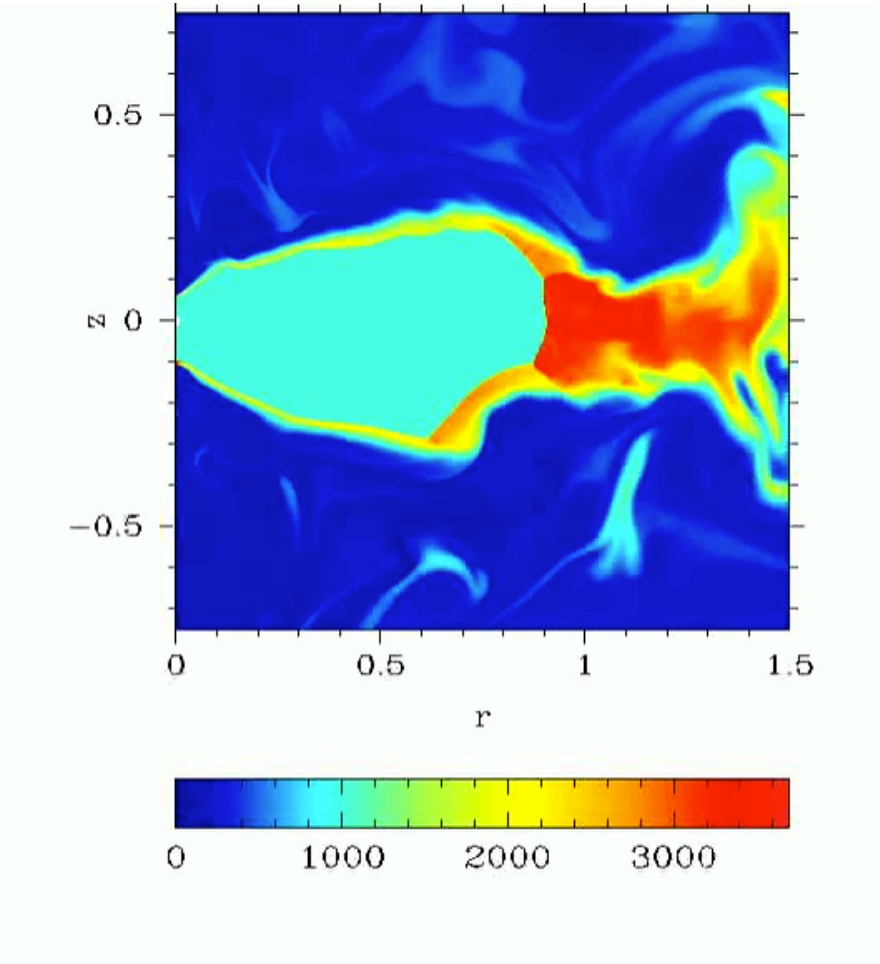

Instability of the shear layers creates eddies at the rim shock

Eddies are advected outward and a toroidal pressure wave is launched

There is no wave reflection from the boundary

Waves reflected on the axis modulate the TS shape

The equatorial channel is kink unstable

MHD variability - Emission

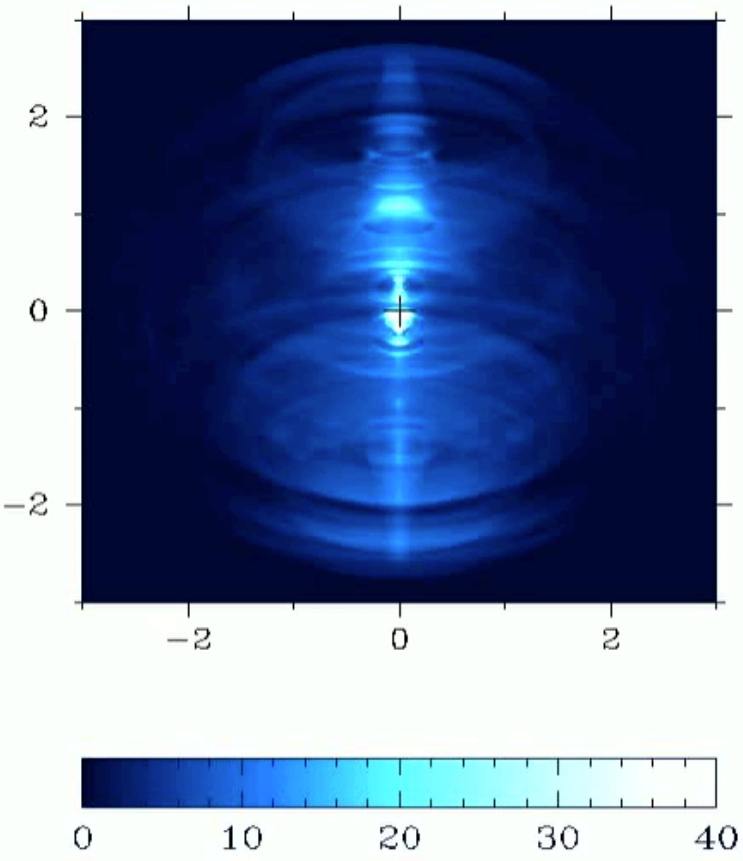

Outgoing wave pattern

Large luminosity variations

Features slow down as they move outward

Variability observed both in the knot and in the sprite

Pressure waves produce variability in the axial emissivity

Large striped wind are favored to produce a bright torus

MHD variability - High Energy

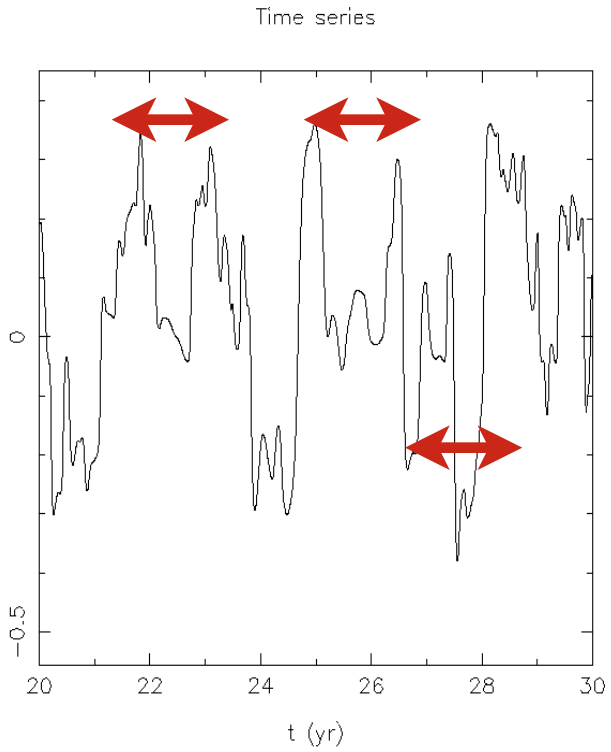

~2yr timescale

HE emission traces the shock dynamics

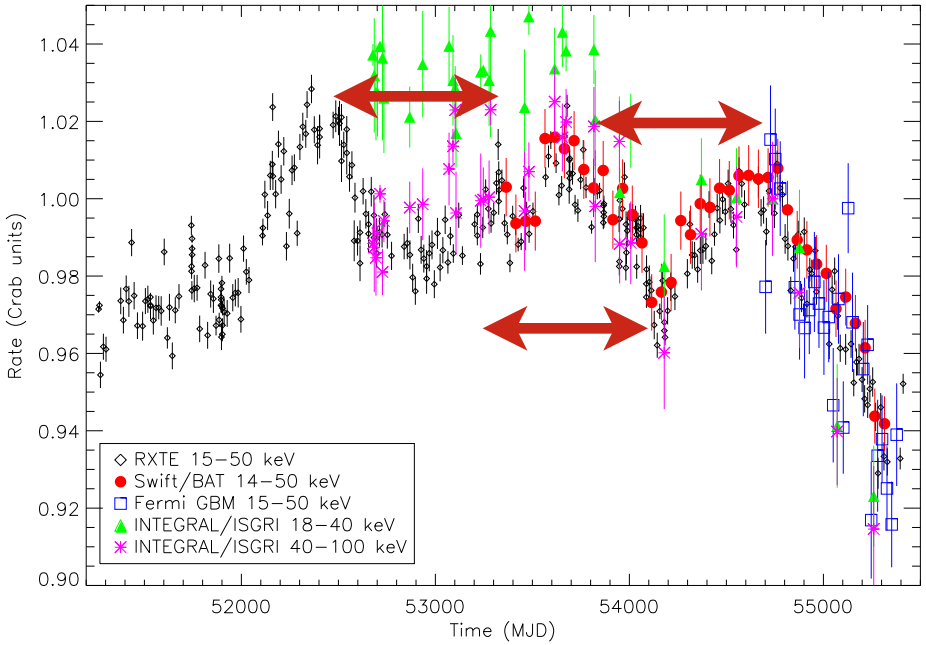

Wilson-Hodge et al. 2010

Variability

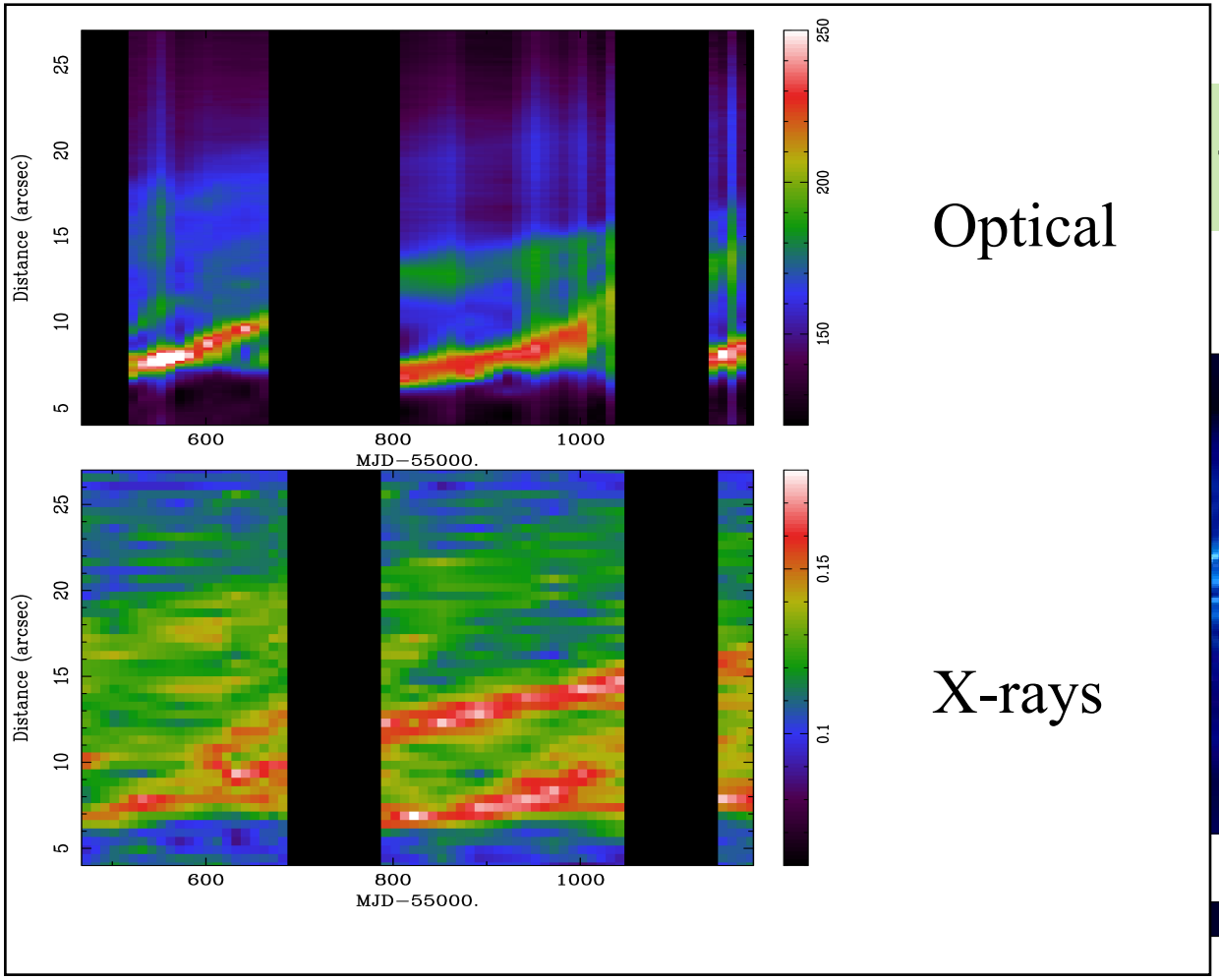

Optical

X-rays

There is a general tendency for outgoing wave pattern

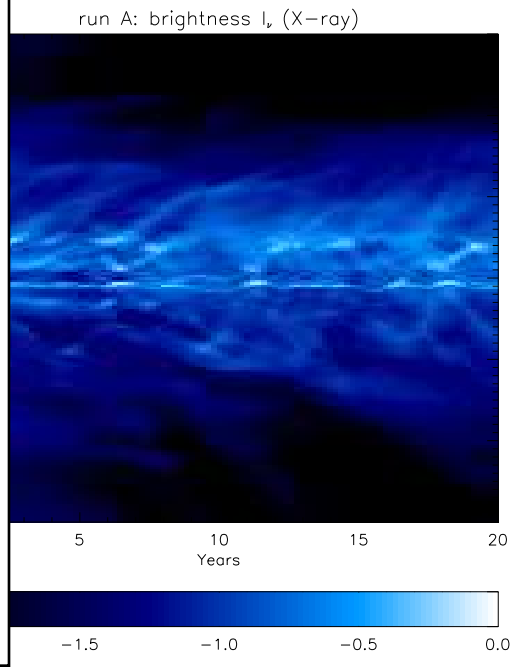

Flares

Not from pulsar :

- flares are not pulsed or in phase
- no variations in the timing residual

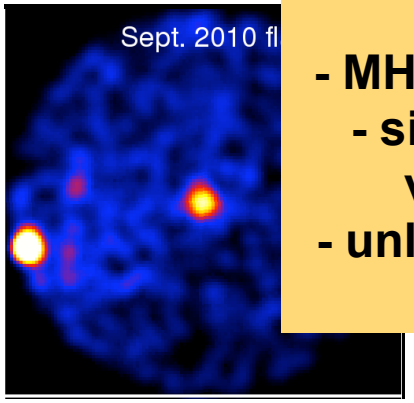

Unlikely MHD origin like the slow variability of the wisps:

- MHD effects are achromatic
- size of the accelerator is very small (day-light)
- unlikely high magnetic field

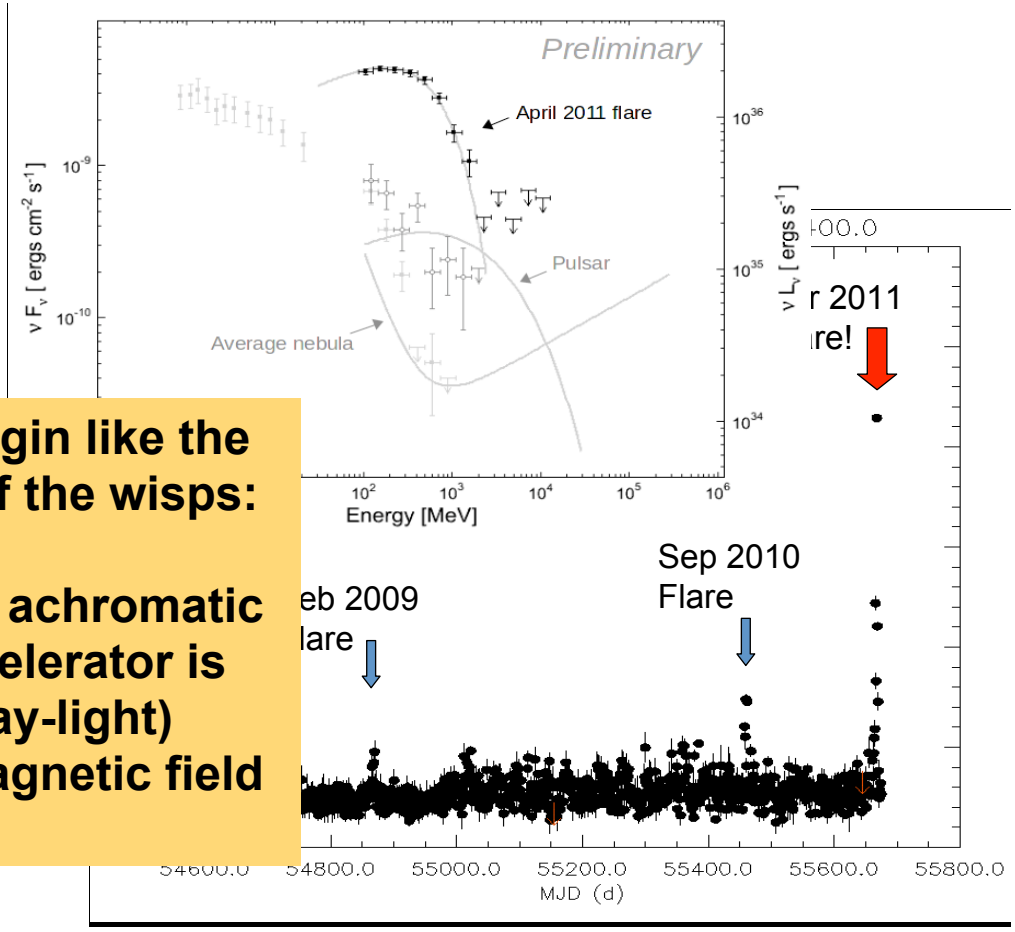

Going 3-D

Configurations with a purely toroidal field are unstable for current driven (kink) instability

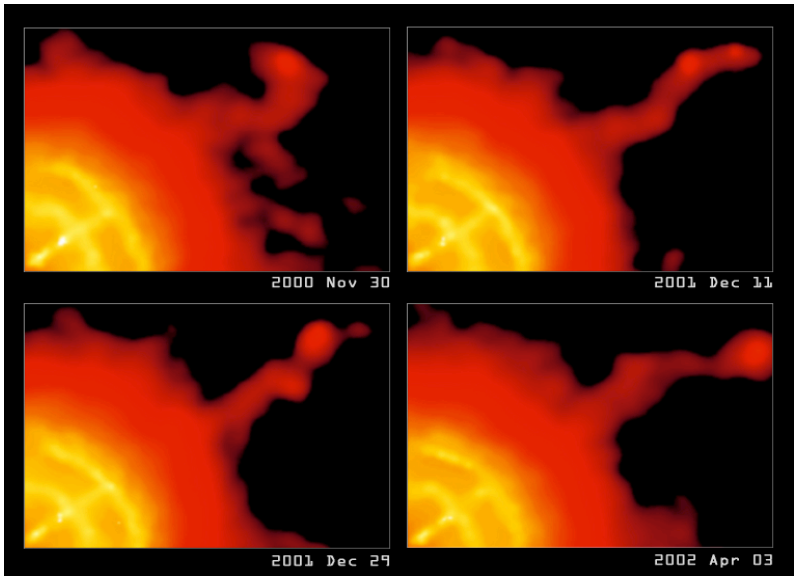

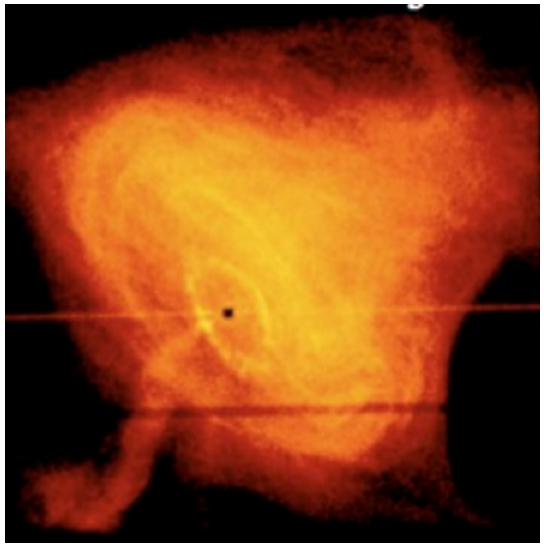

3D vs 2D

3D allows for anisotropy/ asymmetry

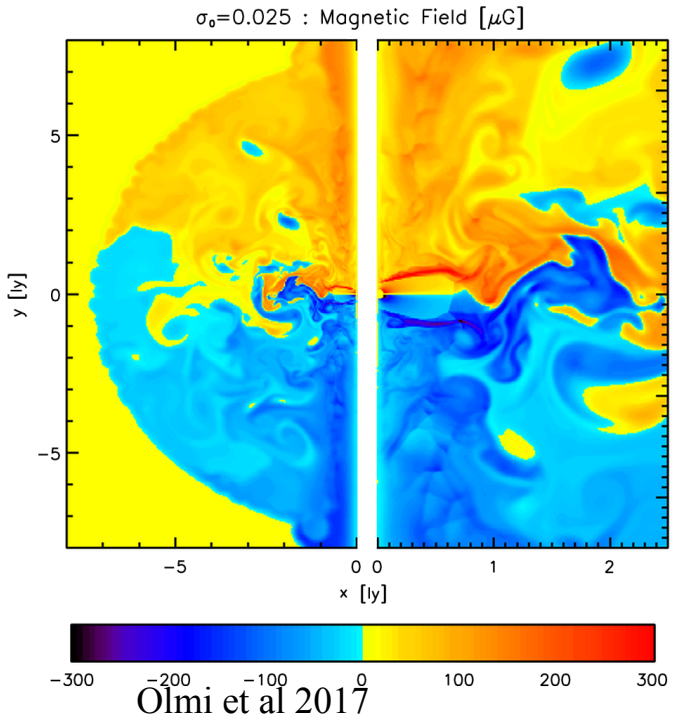

Olmi et al 2017

Inner region still axisymmetric Torus-Jet

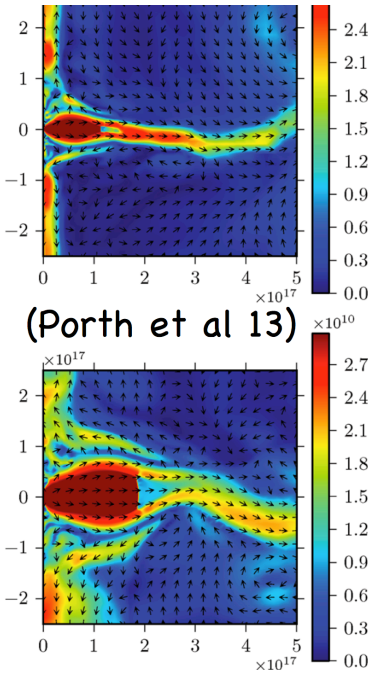

(Porth et al 13)

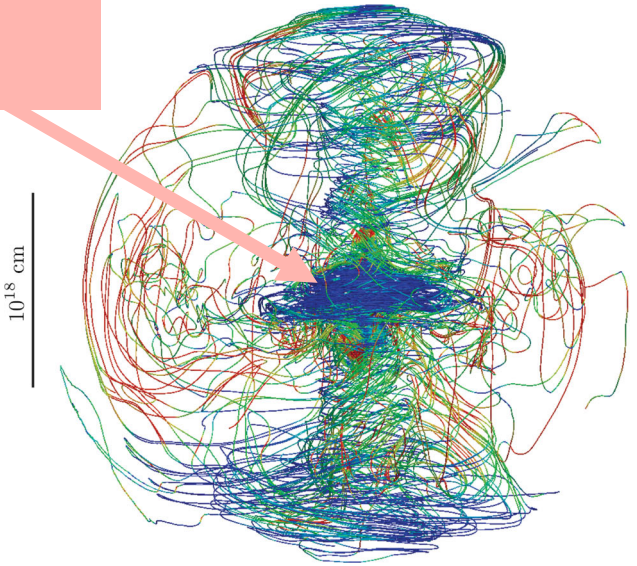

Less ordered field in outer region

Polarized Intensity

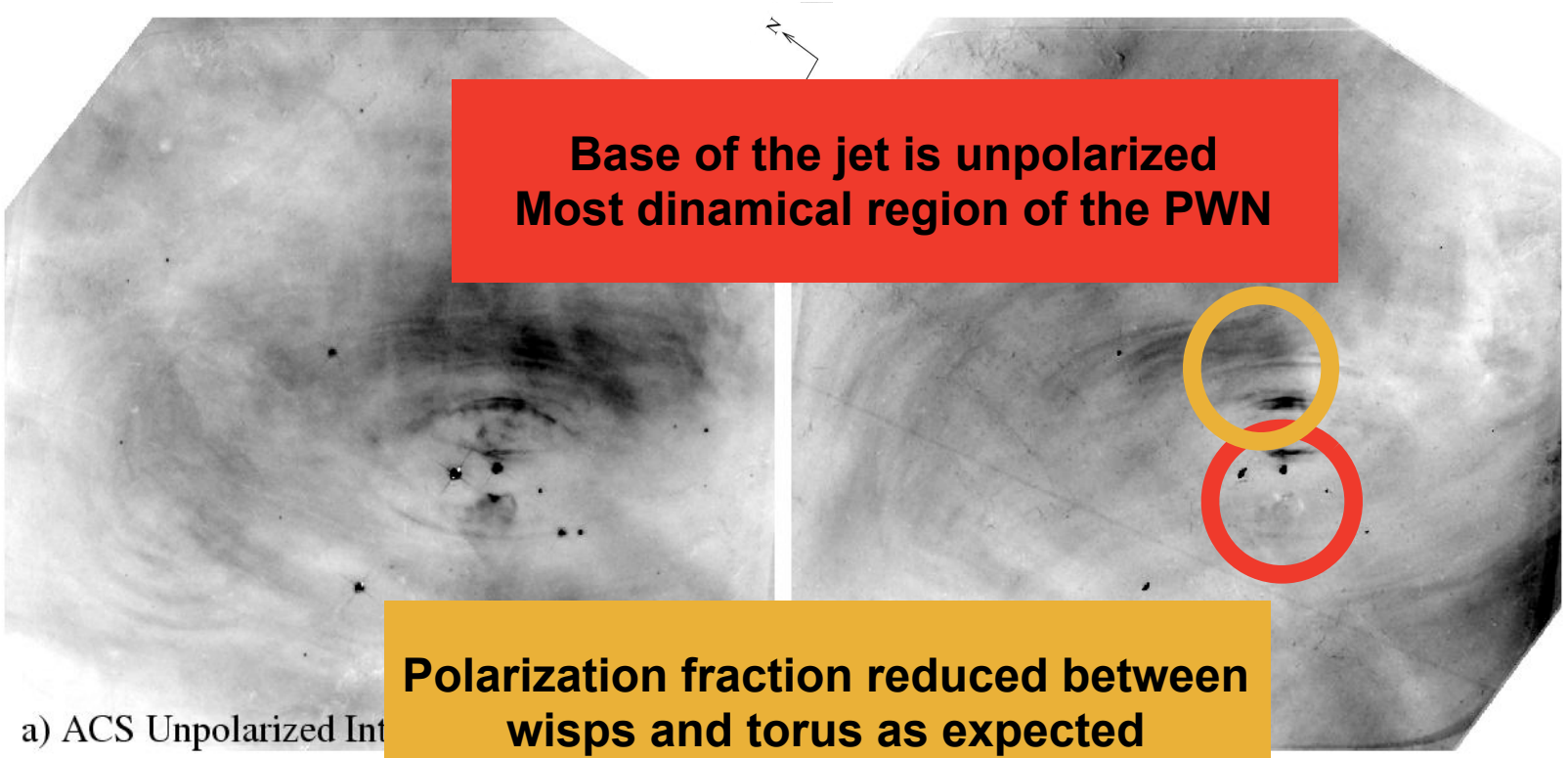

Base of the jet is unpolarized
Most dinamical region of the PWN

Polarization fraction reduced between wisps and torus as expected

Hester 08

Striated aspect of the polarized map
Coherent magnetic field

Optical Measures

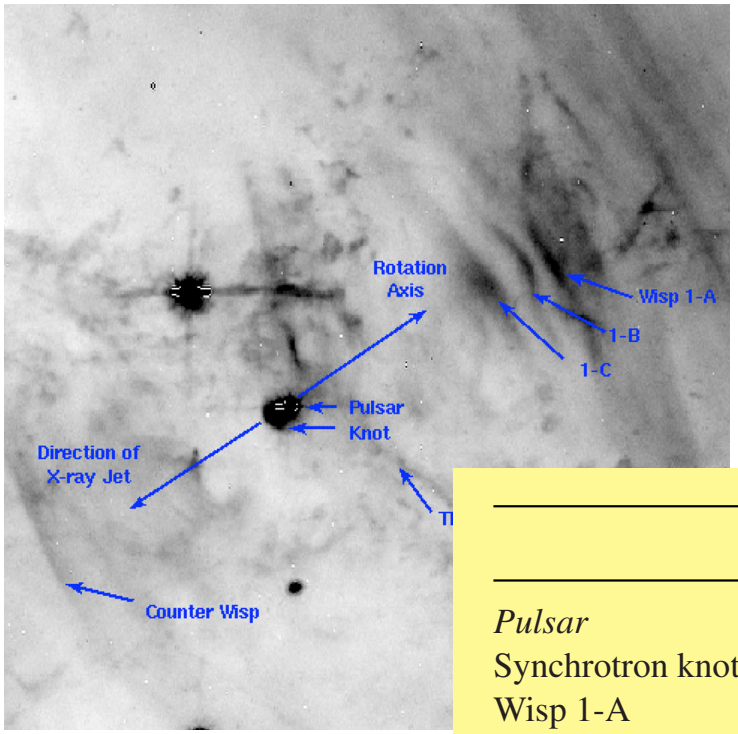

Moran et al 14

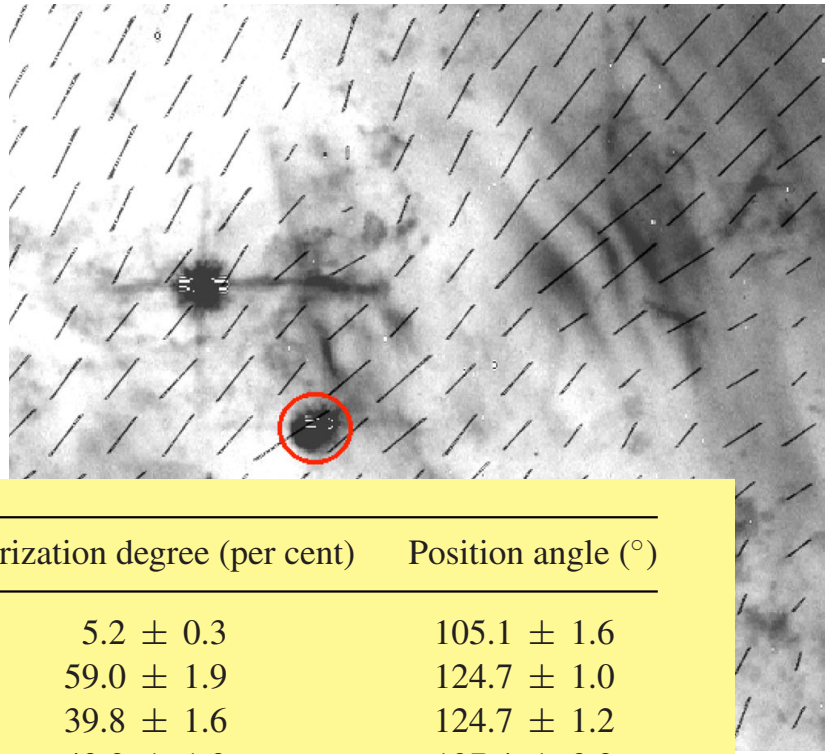

	Polarization degree (per cent)	Position angle (°)
Pulsar	5.2 ± 0.3	105.1 ± 1.6
Synchrotron knot	59.0 ± 1.9	124.7 ± 1.0
Wisp 1-A	39.8 ± 1.6	124.7 ± 1.2
Wisp 1-B	43.0 ± 1.3	127.4 ± 0.9
Wisp 1-C	38.5 ± 1.3	128.8 ± 1.0
Thin Wisp	36.7 ± 1.4	127.1 ± 1.0
Counter Wisp	40.6 ± 1.5	130.3 ± 1.1

Crab X-ray Polarization

TABLE 3

POLARIZATION RESULTS FOR TIME-AVERAGED 1976 AND 1977 OBSERVATIONS WITH AVERAGE EARTH-OCCULTED AND OFF-SOURCE BACKGROUNDS

Parameter*	First Order (2.6 keV)	Second Order (5.2 keV)
$\bar{R}$ (Counts $s^{-1} \times 10^3$)	302.32 ± 1.29	53.13 ± 0.65
Q (%)	13.02 ± 0.65	11.24 ± 1.86
U (%)	−14.10 ± 0.65	−15.94 ± 1.86
P (%)	19.19 ± 0.97	19.50 ± 2.77
ϕ (degrees)	156.36 ± 1.44	152.59 ± 4.04

*See footnote to Table 2.

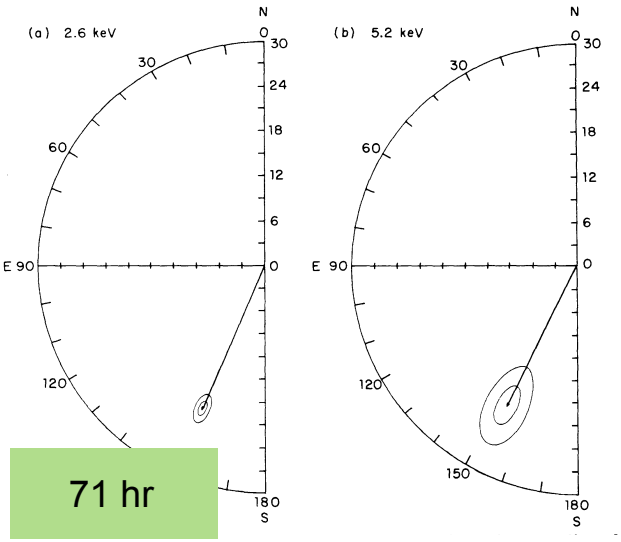

71 hr

Weisskopf et al 1978

Crab nebula is the only source for which there is an X-ray polarization measure - Weisskopf et al. 1978

PF ~ 19%
PA ~155 deg

POGO+ Chauvin et al 2017
PF ~ 21% (20-240keV)
PA ~ 131 deg

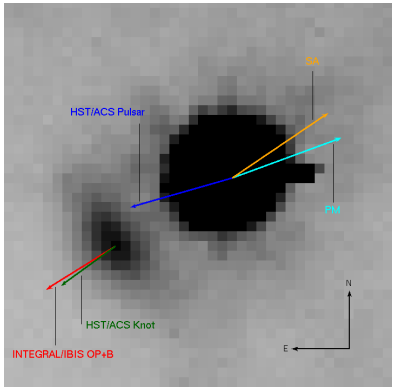

Integral Moran et al 2013
PF ~ 60-90% (300-450keV)
PA ~ 115 deg

SNR -Interaction

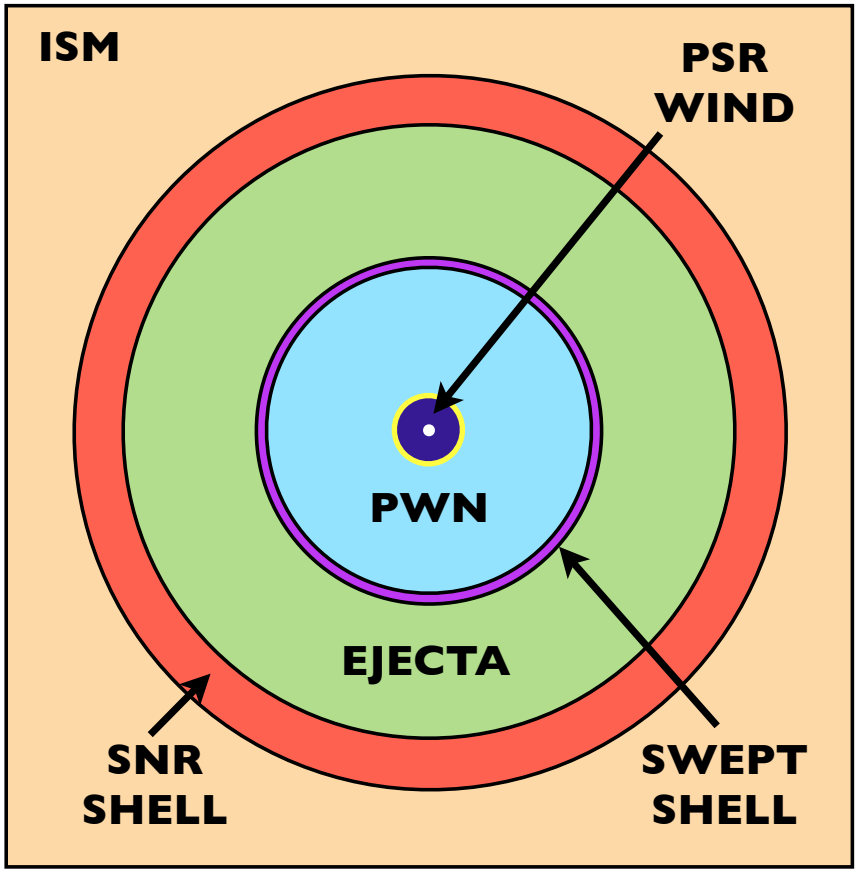

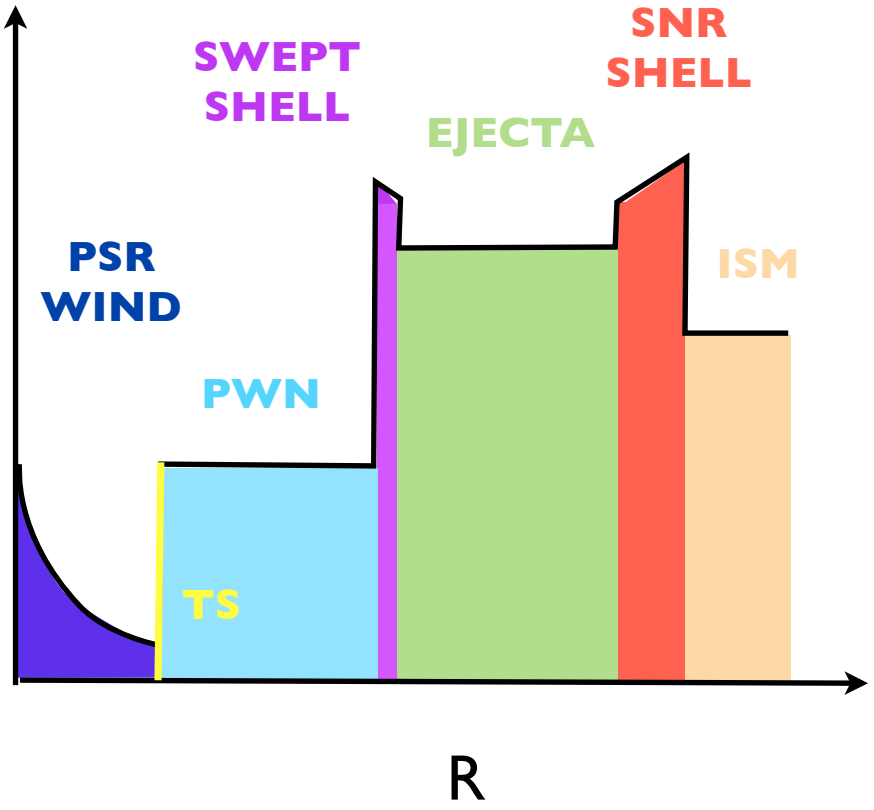

Phase I: Free Expansion in Ejecta

Continuous energy injection - High synchrotron luminosity
PWN expands supersonically, $R_{PWN} \propto t^{6/5}$
Pulsar at the center of PWN

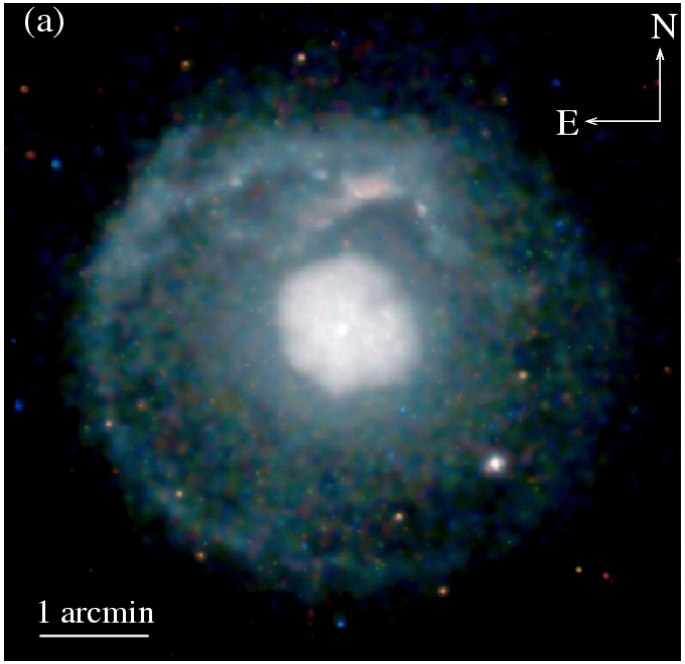

SNR G21.5-0.9 (X-rays)
Matheson & Safi-Harb 2005

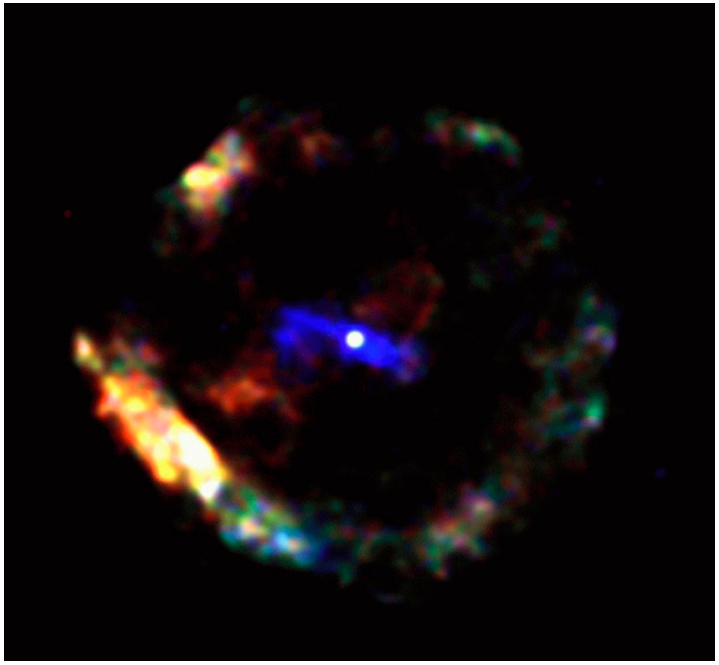

SNR G11.2-0.3 (X-rays)
Kaspi et al. 2001

Pulsar displacement

Reverse interacts with PWN after time $t \sim 7 M_{10 M_{sun}}^{5/6} E_{51}^{-1/2} n_0^{-1/3}$ kyr

Compression; synchrotron burn-off at high energies
Effects of inhomogeneous ISM
Offset pulsar; filamentary structure; mixing

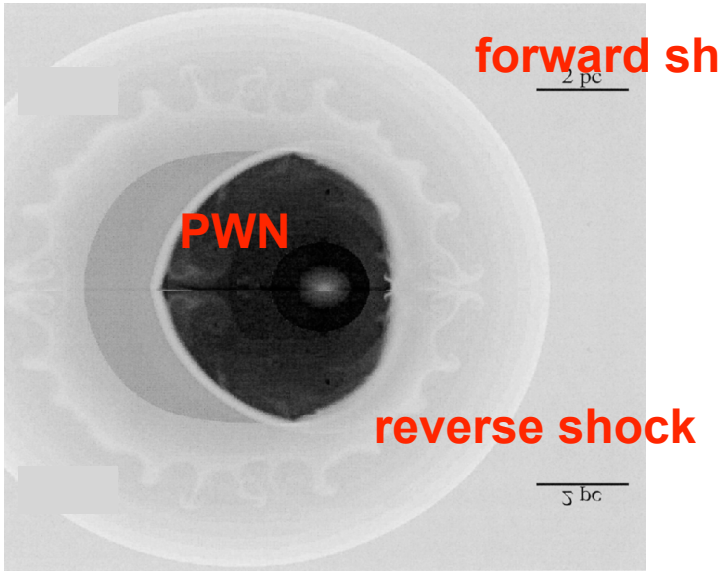

van der Swaluw et al. (2004)

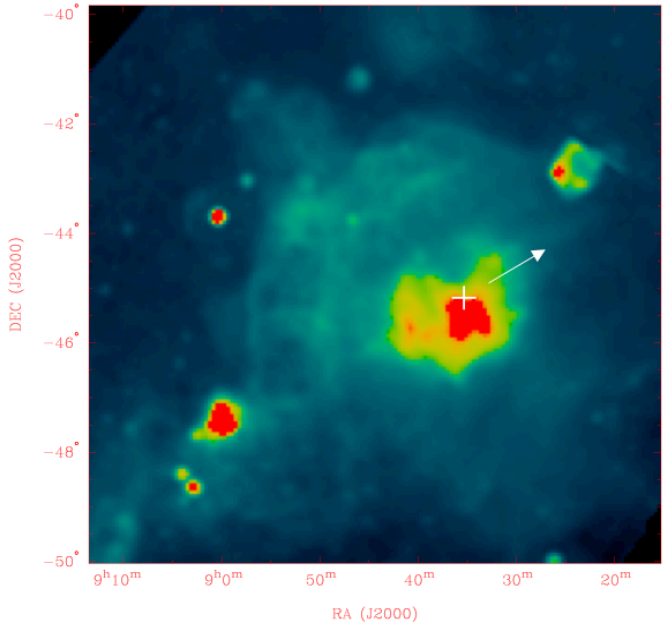

Vela (radio) Duncan et al. 1996

Interaction with SNR Shell

PWN expands into shocked ejecta
"Relic" radio PWN left behind
New PWN around pulsar (X-ray)

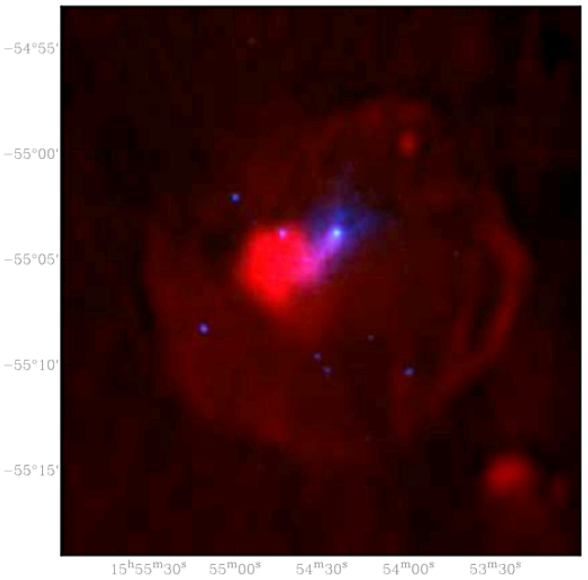

SNR G327.1-1.1, Gaensler & Slane

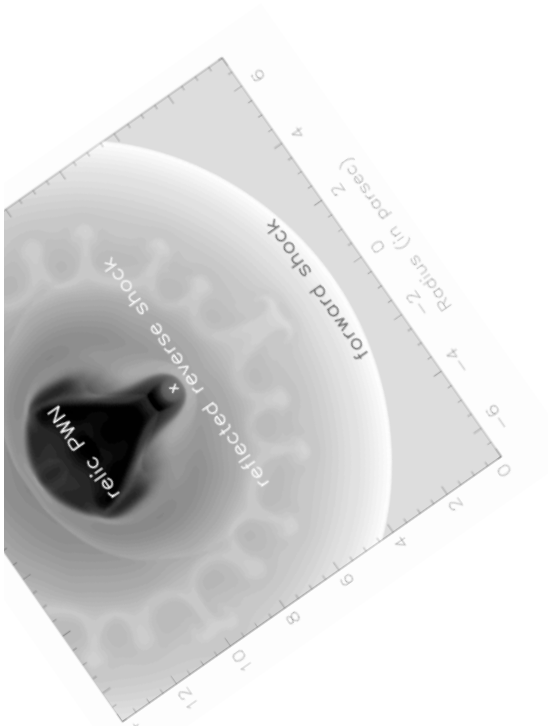

van der Swaluw (2004)

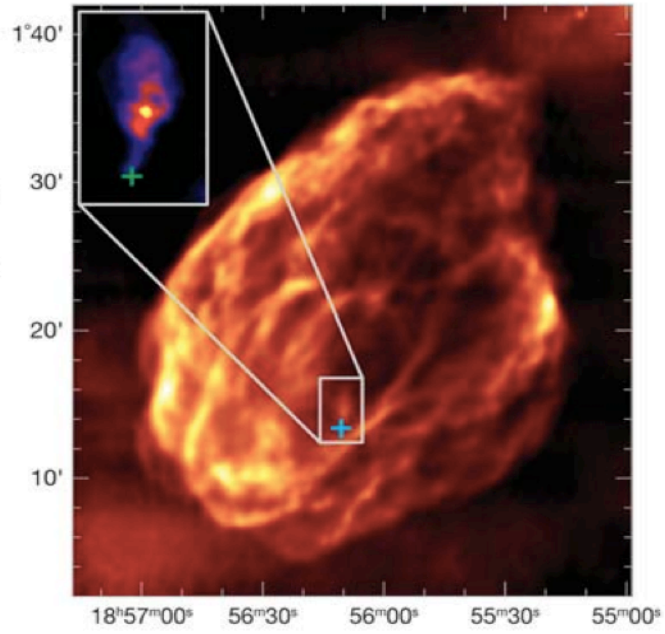

SNR W44 (Frail et al. 1996, Giacani et al. 1997)

SNR Interaction

Mixing with the SNR matter
Rayleigh Taylor instability

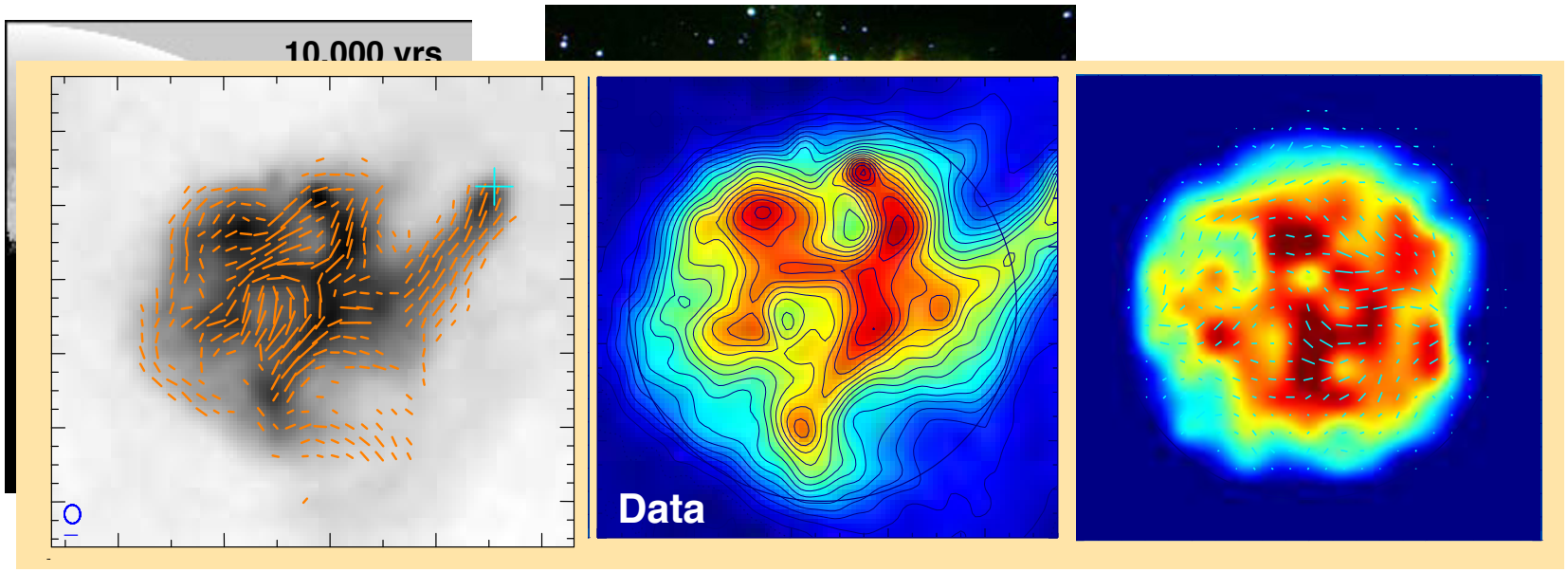

G327 Ma et al. 2015

Phase III : Bow Shock PWN

$$t_{esc} V_{psr} = R_{snr} = \left(\frac{E_{sn}}{\rho_{ism}}\right)^{1/5} t_{esc}^{2/5}$$

$$\Rightarrow t_{esc} \approx \left(\frac{E_{sn}}{\rho_{ism}}\right)^{1/3} \left(\frac{1}{V_{psr}}\right)^{5/3} \approx 2 \times 10^5 \mathrm{yr} \left(\frac{E_{sn}}{10^{51}\mathrm{erg}}\right)^{1/3} \left(\frac{V_{psr}}{200\mathrm{km\ s}^{-1}}\right)^{5/3} \left(\frac{n_{ism}}{1\mathrm{cm}^{-3}}\right)^{-1/3}$$

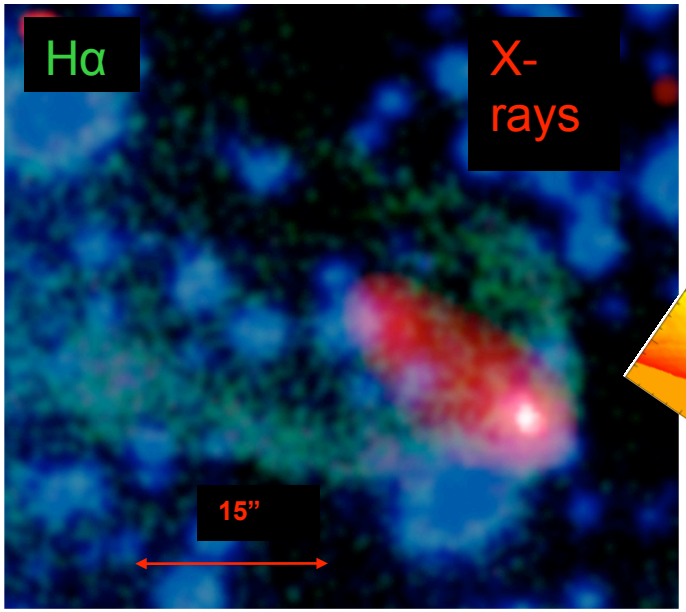

PSR B1957+20 (Stappers et al. 2003)

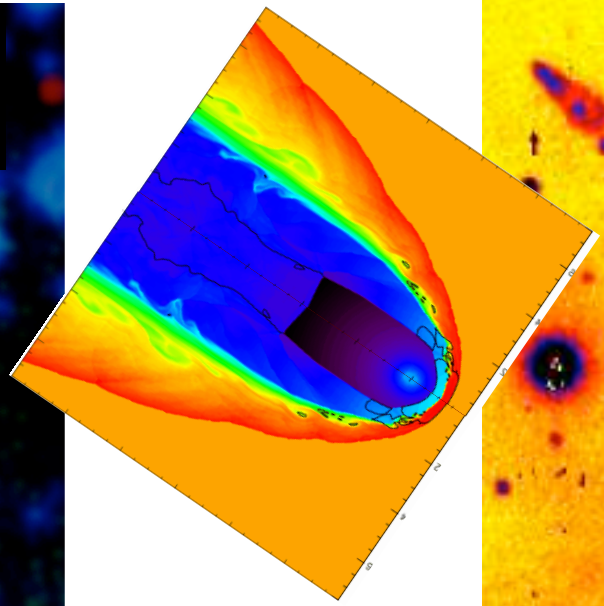

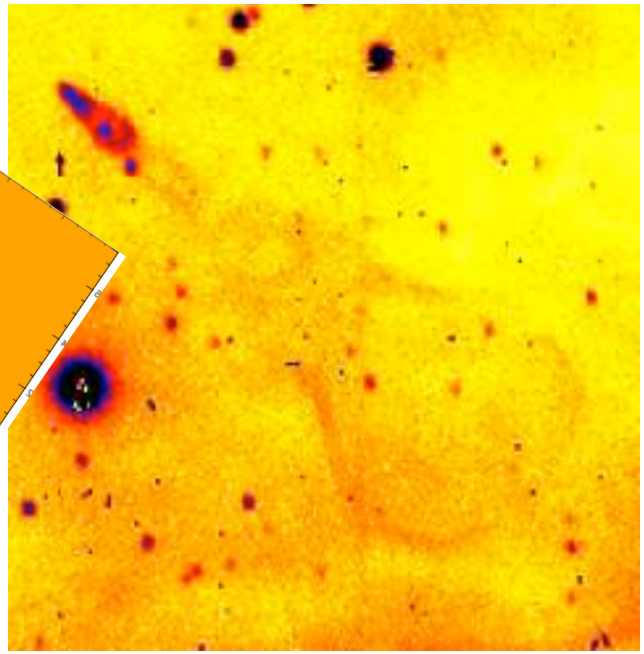

PSR B2224+65 (Chatterjee & Cordes 2002)

Particle Escape

The are BS PWNe where the X-ray "tail" is where it should not be!

The particles in these features are ~ PSR voltage

PSR J1101 (Pavan et al 2016)

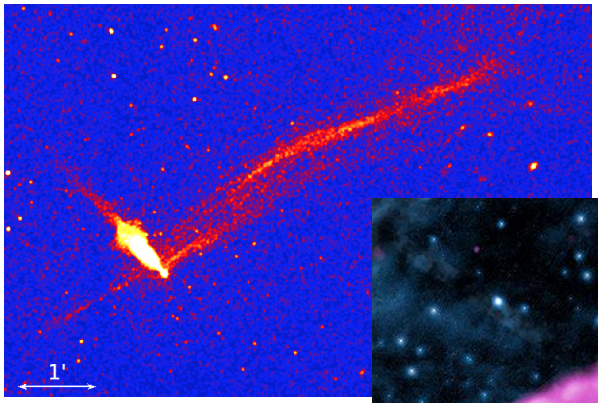

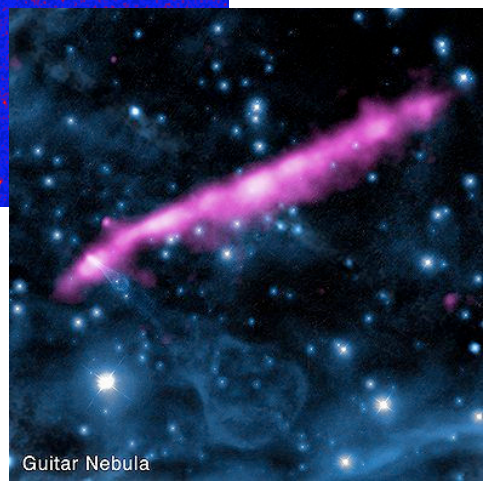

Guitar (Wong et al 2003)

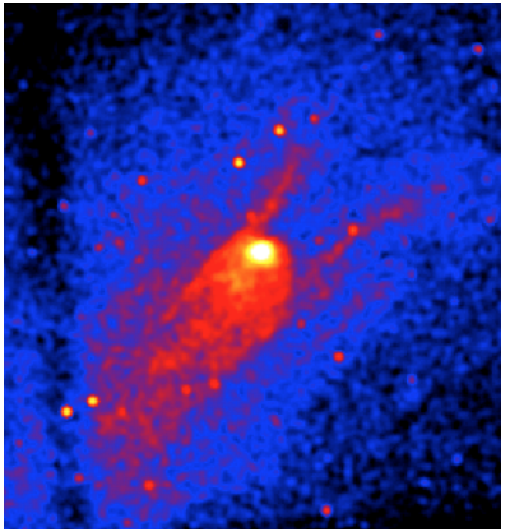

G327 (Temin et al 2009)

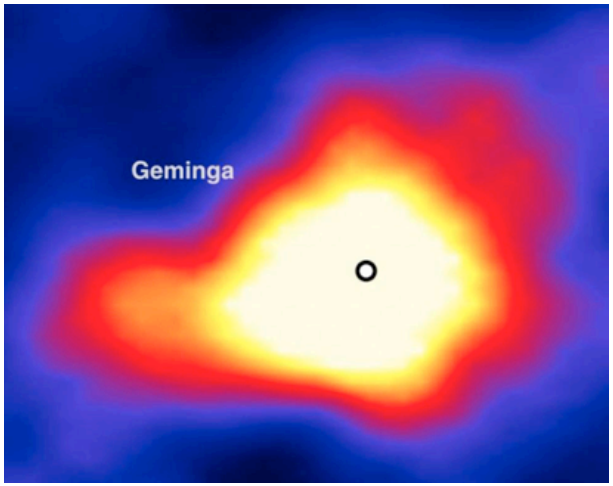

Geminga (HAWC Abeysekara et al 2017)

TeV halo suggest strong diffusion

Bow-Shock

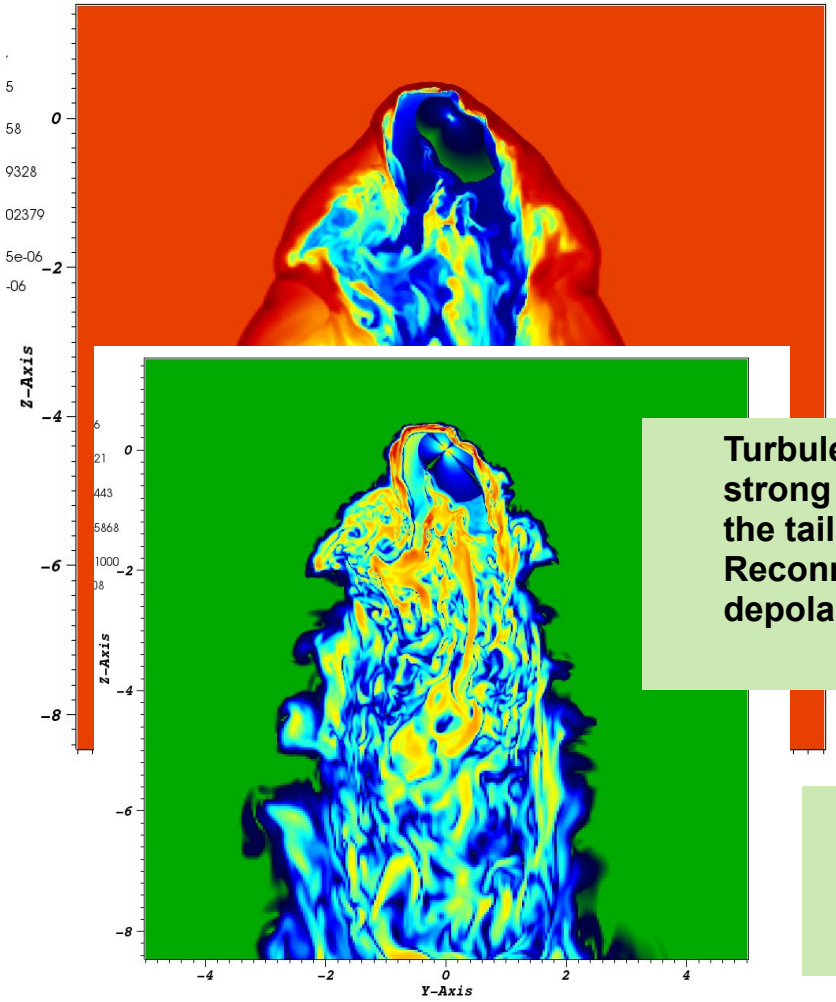

BSPWNe are intrinsically 3D objects
Shape of bow shock - inclination

Turbulence lead to strong currents in the tail
Reconnection and depolarisation

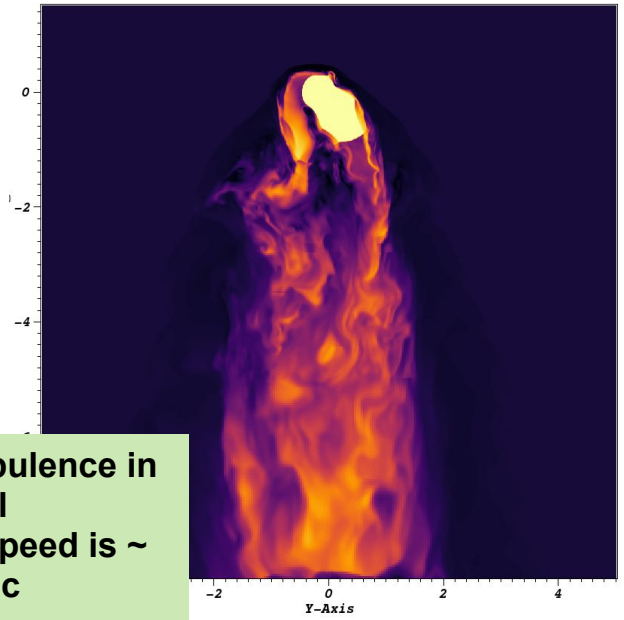

Mixing and turbulence in the tail
Average flow speed is ~ 0.6/0.8 c

Older systems

Older systems show a displacement of the TeV gamma emission from the pulsar: reverberation, bow-shock

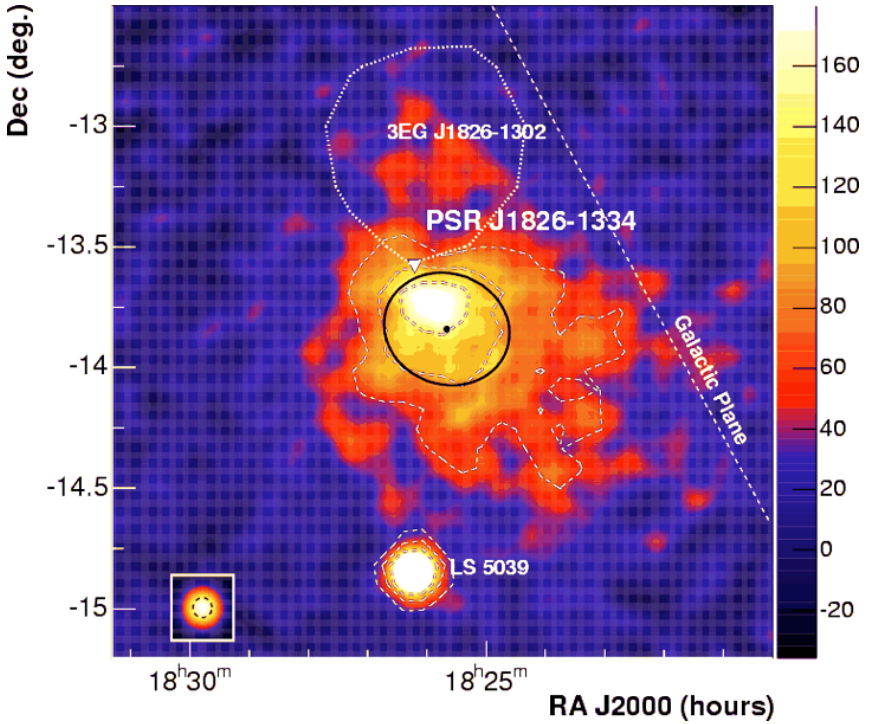

J1825-137 (HESS; Aharonian et al. 2005)

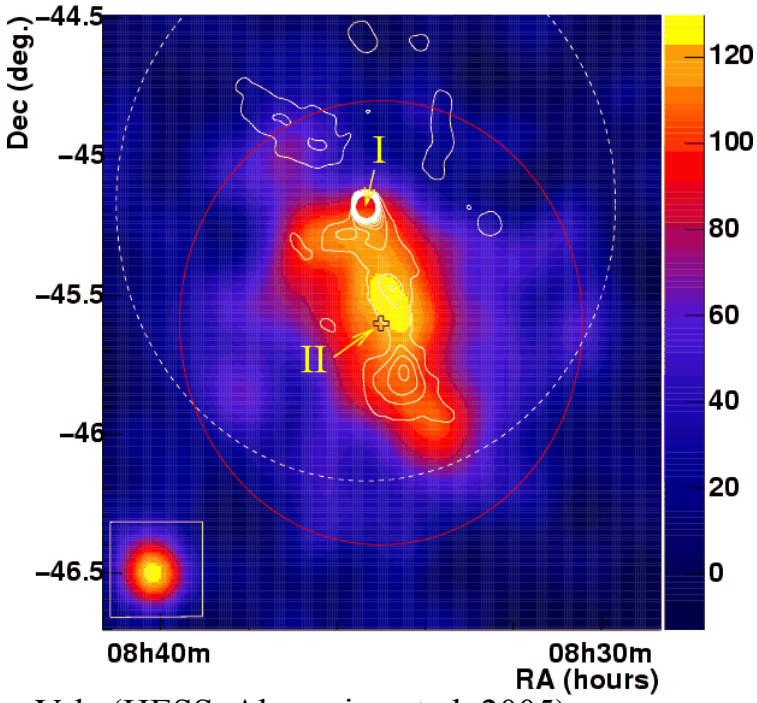

Vela (HESS; Aharonian et al. 2005)

IXPE

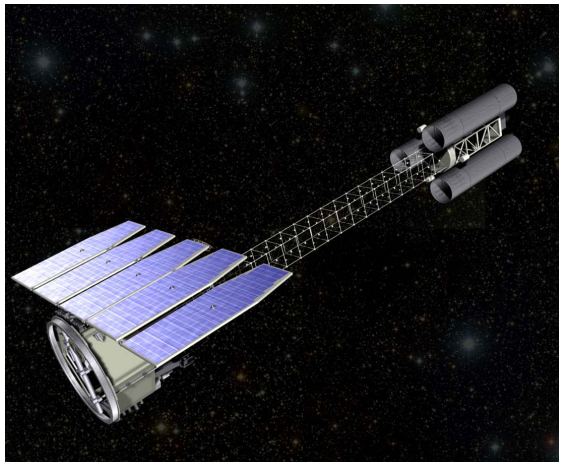

IXPE is a new x-ray polarimetric satellite scheduled to launch in 2022

It operates in almost the same energy band of CHANDRA 2-8 keV

5.2’ FOV - 30” res

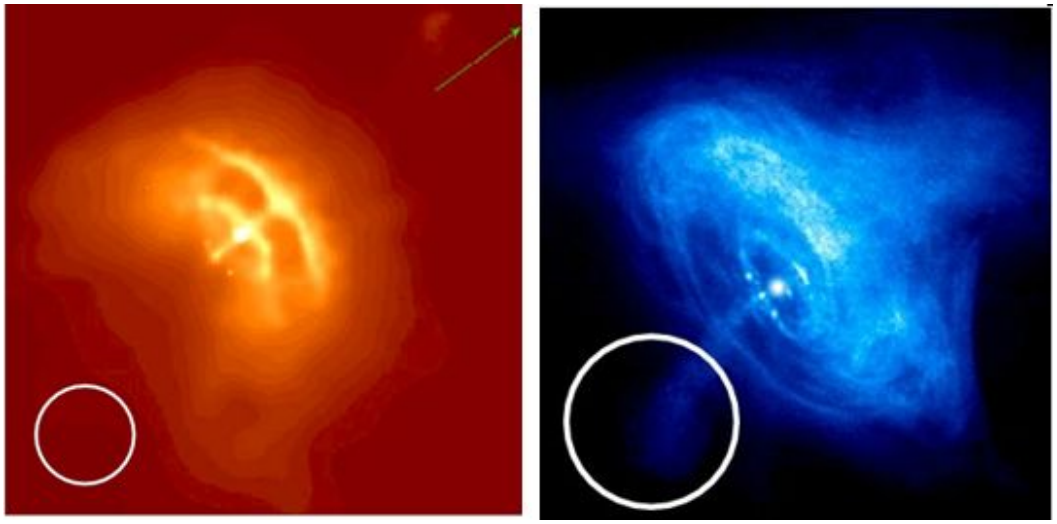

Crab X-ray Polarization

TABLE 3

POLARIZATION RESULTS FOR TIME-AVERAGED 1976 AND 1977 OBSERVATIONS WITH AVERAGE EARTH-OCCULTED AND OFF-SOURCE BACKGROUNDS

Parameter*	First Order (2.6 keV)	Second Order (5.2 keV)
$\bar{R}$ (Counts $s^{-1} \times 10^3$)	302.32 ± 1.29	53.13 ± 0.65
Q (%)	13.02 ± 0.65	11.24 ± 1.86
U (%)	−14.10 ± 0.65	−15.94 ± 1.86
P (%)	19.19 ± 0.97	19.50 ± 2.77
ϕ (degrees)	156.36 ± 1.44	152.59 ± 4.04

*See footnote to Table 2.

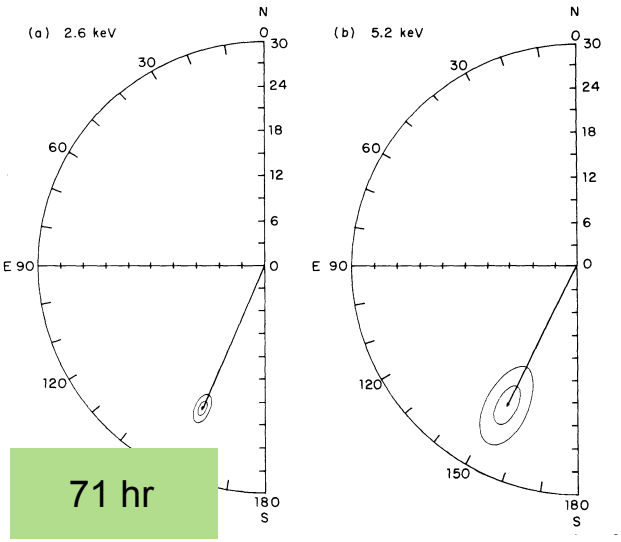

71 hr

Weisskopf et al 1978

Crab nebula is the only source for which there is an X-ray polarization measure - Weisskopf et al. 1978

PF ~ 19%
PA ~155 deg

POGO+ Chauvin et al 2017
PF ~ 21% (20-240keV)
PA ~ 131 deg

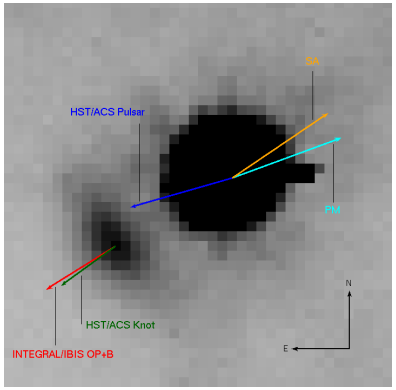

Integral Moran et al 2013
PF ~ 60-90% (300-450keV)
PA ~ 115 deg

MSH 15-52

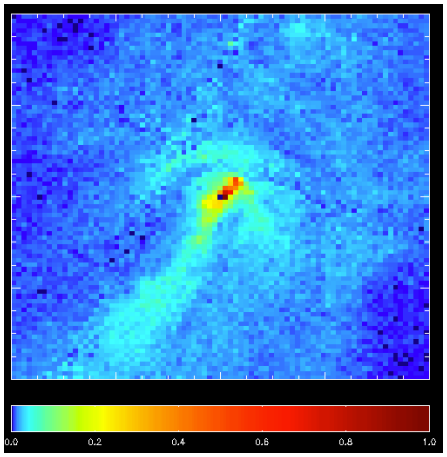

Jet Dominated system

Variability in the jet

Nature of variability on magn. geometry

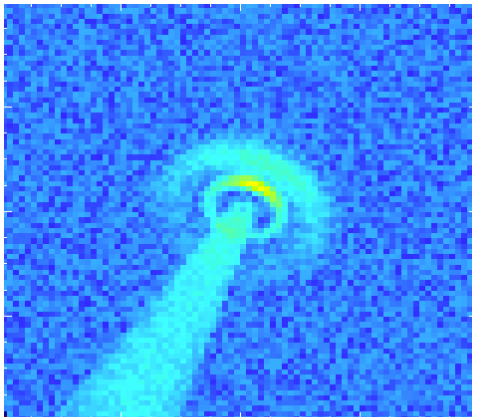

Radial

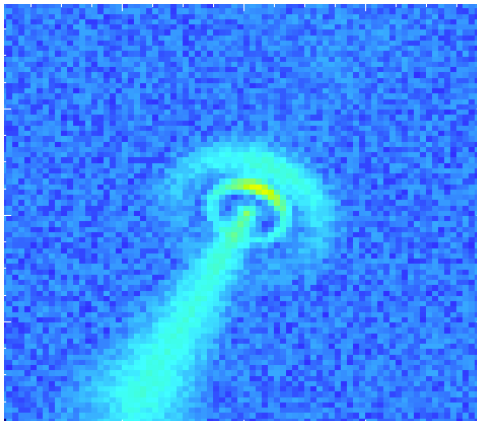

Toroidal

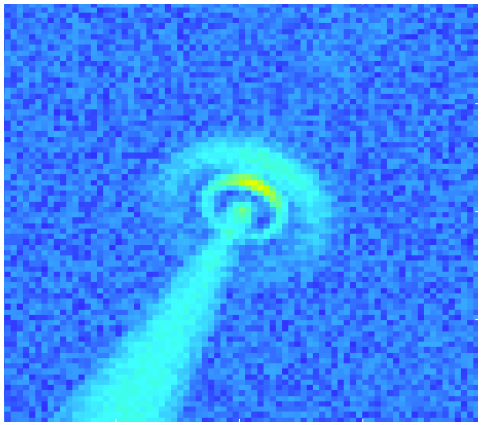

Random

Summary and conclusions

- PWNe can be though as calorimeters and imagers for the pulsar wind
- 1-zone models provide good SED fitting
- 2D-MHD models successful in reproducing the X-ray features
- 3D-MHD still hard to do - may be able to bridge the gap between the previous ones
- Acceleration at the TS (?) still poorly understood
- Older systems have been investigated only partially and there are few results
- BSPWNe could be one of the main contributor to galactic positrons

Thank you